Nanosilver fluoride-coated orthodontic elastomerics for inhibition of biofilm formation and demineralization

Jun-Hyuk Choi

The Graduate School

Yonsei University

Department of Applied Life Science

Nanosilver fluoride-coated orthodontic elastomerics for inhibition of biofilm formation and demineralization

Directed by Professor Baek-Il Kim

A Dissertation
Submitted to the Department of Applied Life Science
And the Graduate School of Yonsei University
in partial fulfillment of the requirements
for the degree of Doctor of Philosophy in Dentistry

Jun-Hyuk Choi

June 2024

This certifies that the Doctoral Dissertation of
Jun Hyuk Choi is approved.

Thesis Supervisor: Baek-Il Kim

Thesis Committee: Ho-Keun Kwon

Thesis Committee: Ki-Ho Chung

Thesis Committee: Hoi-In Jung

Thesis Committee: Chung-Min Kang

The Graduate School
Yonsei University
June 2024

Acknowledgements

예방치과학교실에서 보낸 지난 5년은 무엇과도 바꿀 수 없는 값진 시간이었습니다. 이 시간을 마무리하며, 논문이 완성될 수 있도록 큰 도움을 주신 모든 분께 깊은 감사의 인사를 올립니다.

우선 김백일 지도교수님께 진심으로 감사드립니다. 부족한 제자를 믿어주시고, 개인적 발전과 학문적 성장을 위해 방향을 제시해 주신 덕분에 어려운 순간들을 잘 극복할 수 있었습니다. 또한, 넓은 시야로 세상을 바라볼 수 있도록 이끌어주신 권호근 교수님께 감사의 말씀을 드립니다. 연구적인 부분뿐만 아니라 연구 외적인 부분까지 세심하게 지도해 주신 정회인 교수님께 깊이 감사드립니다. 완성도 있는 논문이 될 수 있도록 사려 깊은 조언을 해주신 정기호 교수님께 감사드립니다. 논문 전반에 걸쳐 아낌없는 제언을 해주신 강정민 교수님께 감사드립니다. 학부 때부터 따뜻한 격려와 조언을 해주신 한선영 지도교수님께도 감사의 마음을 전달해 드립니다. 또한 학위 과정의 기반을 마련해 주신 정원균 교수님, 김남희 교수님, 노희진 교수님, 문소정 교수님께 감사의 인사를 드립니다.

지난 5년 동안의 학위과정은 좋은 선생님들과 함께했기에 더욱 특별했습니다. 연구 전반에 걸쳐 많은 영감을 주신 Dr. Elbert, 실험과 연구

분야에 대해 깊이 있는 가르침을 주신 강시묵 교수님, 연구의 시작부터 함께 고민해 주시고 항상 큰 힘이 되어주신 이은송 교수님께 감사드립니다.
교실생활 전반에 걸쳐 많은 도움을 주신 이형석, 정은하, 이주영, 김상겸, 박석우, 김효정, 김은수, 조무열 선배님과 김별, 박솔, 이채현, 정주현, 김아름, 조연지, 차현재, 양정우, 최아현, 포은, 김채연 선생님께도 감사드립니다. 항상 따뜻한 말로 격려해 주신 남상미, 맹유진, 황혜림, 이선영, 전미경, 국혜진, 정명진, 김예슬, 황지현 선생님께 감사드립니다.

가족들에게도 깊은 감사의 마음을 전합니다. 꿈을 향한 여정에서 물심양면으로 지원해 주시고 믿어주신 부모님, 손자를 위해 기도해 주신 할머니, 힘들 때마다 위로와 격려를 아끼지 않았던 누나 감사드립니다.

주변의 도움이 없었다면 오늘의 성과는 이루어질 수 없었을 것입니다. 저를 믿고 응원해 주신 모든 분께 깊은 감사의 인사를 드립니다.

2024년 6월, 최준혁 올림

CONTENTS

List of Figures

List of Tables

Abstract

Nanosilver fluoride-coated orthodontic elastomerics for inhibition of biofilm formation and demineralization

Jun-Hyuk Choi

Department of Applied Life Science

The Graduate School, Yonsei University

(Directed by professor Baek-Il Kim)

In orthodontic treatment, biofilms are easily formed around orthodontic brackets and are difficult to remove, increasing the risk of dental caries. Thus, this study developed a nano silver fluoride sustained-release orthodontic elastomerics (NSF-RE), to prevent biofilm accumulation and white spot lesions (WSLs) formation around orthodontic

brackets, and assessed its chemical and physical properties, along with its anti-biofilm and demineralization-inhibiting effect for clinical applications.

The first objective of this study was to identify the optimal coating solution conditions for sustained release of silver nanoparticles (AgNPs), fluoride and to evaluate its physical properties. The second objective was to assess the antimicrobial persistence and anti-biofilm effects against *Streptococcus mutans* (*S. mutans*), and the third objective was to evaluate the anti-biofilm and demineralization-inhibiting effects on a multispecies biofilm model.

In the first study, orthodontic elastomerics were coated with four different combinations of ethyl cellulose and polyethylene glycol, mixed in varying compositions, using a dip-coating method. The release amount and duration of AgNPs and fluoride from the coated elastomerics, along with the compatibility of the tensile force with orthodontic brackets, was evaluated. Elastomerics coated with solutions containing ethyl cellulose demonstrated sustained release of both AgNPs and fluoride for 7 days. Cumulative release for 7 days showed that elastomerics coated with a 2:1 ratio of ethyl cellulose to polyethylene glycol (NSF-EP2) exhibited significantly higher cumulative release compared to other groups ($P < 0.01$). Tensile forces were not significantly different among groups.

The second study evaluated the antimicrobial persistence and anti-biofilm effects of the coated elastomerics against *S. mutans*. The antibacterial effect was assessed by placing

the elastomerics on *S. mutans*-inoculated agar plates, incubating for 24 h, and then transferring the elastomerics to fresh agar plates daily for 7 days. The inhibition zone was measured. The anti-biofilm effect was evaluated by quantifying the colony forming units (CFUs) and analyzing the biofilm thickness and live/dead cell ratio using confocal laser scanning microscopy (CLSM) after 64 h of biofilm maturation. NSF-EP2 showed the largest inhibition zone, significantly larger than NSF and NSF-E by 2.64 and 1.31 times, respectively ($P < 0.001$ and $P < 0.001$, respectively). NSF-EP2 also had 57% lower CFUs compared to the control ($P < 0.001$). CLSM results indicated that NSF-EP2 significantly reduced biofilm thickness by 83% and live/dead cell ratio by 96% compared to the control ($P < 0.001$), showing the highest anti-biofilm effect among the groups.

The third study assessed the anti-biofilm and demineralization-inhibiting effects of NSF-RE using a multi-species dental biofilm model. Biofilm was formed on bovine enamel specimens, and biofilm maturity was evaluated daily for 7 days using quantitative light-induced fluorescence (QLF) to measure the red/green ratio (R/G ratio). After 7 days of biofilm formation, cell viability was assessed using CFUs, and biofilm thickness and live/dead cell ratio were evaluated using CLSM. Microbial composition changes were analyzed on days 3 and 7 using next-generation sequencing (NGS). Demineralization inhibition was evaluated by measuring mineral loss (ΔF, ΔF_{max}) in enamel beneath the biofilm using QLF. The effective range of released substances from the elastomerics was assessed by measuring enamel $\Delta\Delta F$ at varying distances from the elastomerics. NSF-EP showed a significantly lower R/G ratio than the control from day 3 ($P = 0.013$). CFUs

analysis showed a 9.4% reduction in total bacteria and a 13.0% reduction in aciduric bacteria compared to the control (P = 0.001 and P = 0.04, respectively). CLSM results showed a 36.1% reduction in biofilm thickness (P = 0.036), with no significant difference in live/dead cell ratio. The sum of relative abundance of five bacteria associated with dental caries (*S. mutans*, *L. fermentum*, *V. dispar*, *V. atypica*, *V. parvula*) was lowest in NSF-EP. NSF-EP significantly increased ΔF and ΔF_{max} by 34.8% and 38.7%, respectively, compared to the control (P < 0.001 and P = 0.001, respectively). There was no significant difference in ΔΔF at different distances from the elastomerics. NSF-EP, which had the highest cumulative release of AgNPs and fluoride, showed the greatest anti-biofilm and demineralization-inhibiting effects in all evaluations.

In conclusion, NSF-RE containing ethyl cellulose demonstrated anti-biofilm and demineralization-inhiniting effects by continuously releasing AgNPs and fluoride for 7 days, indicating its potential effectiveness in preventing WSLs formation during orthodontic treatment.

Key words: Nano silver fluoride, Drug delivery system, Anti-caries, Orthodontic elastomerics

Nanosilver fluoride-coated orthodontic elastomerics for inhibition of biofilm formation and demineralization

Jun-Hyuk Choi

Department of Applied Life Science

The Graduate School, Yonsei University

(Directed by professor Baek-Il Kim)

1. Introduction

Dental biofilm is formed by the colonization of oral microorganisms on the tooth surface. In stagnant sites where proper oral hygiene is not maintained, dental biofilm accumulates, leading to dental caries and periodontal diseases (Marsh and Bradshaw 1995). Orthodontic

treatment can restore oral function and aesthetics in adolescents and adults, but the various fixed appliances facilitate the accumulation of dental biofilm around them (Topaloglu-Ak et al. 2011). Consequently, approximately 60% of orthodontic patients experience one or more dental biofilm-related diseases post-treatment, with around 15% developing dental caries that require professional care (Ren et al. 2014). Notably, the prevalence of white spot lesions (WSLs) in orthodontic patients is reported to be 30.0-70.0%, significantly higher than the 15.5-40.0% observed in non-orthodontic patients (Heymann and Grauer 2013). WSLs in orthodontic patients often progress to cavities necessitating restoration, highlighting the need for meticulous oral hygiene to manage the biofilm accumulation around fixed orthodontic appliances (Chapman et al. 2010; Kang et al. 2017).

One month after the initiation of orthodontic treatment, the oral microbiota shifts from normal flora to pathogenic gram-negative bacteria. Additionally, the levels of *Streptococcus mutans* (*S. mutans*) and *Lactobacillus* known causative agents of dental caries, increase (Lucchese et al. 2018). Consequently, numerous studies recommend the use of chemical oral hygiene methods, such as mouthwashes, to prevent dental biofilm-related diseases in orthodontic patients (Haas et al. 2014; Pithon et al. 2015). Mouthwashes offer clinical benefits by reducing bacterial load in saliva; however, their antibacterial efficacy against mature dental biofilm is limited (Marsh 2010; Zaura-Arite, Van Marle, and Ten Cate 2001). Furthermore, a single application of mouthwashes cannot inhibit biofilm maturation (Han et al. 2019; Mao et al. 2022). Therefore, to effectively prevent WSLs formation in orthodontic patients, novel anti-biofilm strategies beyond conventional

mouthwash antibacterial therapies are necessary.

A drug delivery system (DDS) is a method for efficiently delivering drugs to target areas and has recently been applied in dentistry as a chemical oral hygiene method (Liang et al. 2020). In orthodontics, various elastomerics that release antibacterial agents have been developed to inhibit dental biofilm formation around brackets (Jeon et al. 2015; Storie, Regennitter, and Vonfraunhofer 1994). However, fluoride-releasing elastomerics are controversial due to their low antibacterial efficacy (Miura et al. 2007; Sudjalim, Woods, and Manton 2006), and elastomerics releasing chlorhexidine (CHX) has side effects potentials such as tooth staining, change in taste of food, and oral mucosal irritation with long-term use (Al-Tannir and Goodman 1994; Choi et al. 2022). Therefore, utilizing anti-caries agents that can overcome these limitations of existing antibacterial elastomers would more effectively prevent WSLs formation in orthodontic patients.

Nano silver fluoride (NSF) is an anti-caries agent composed of silver nanoparticles (AgNPs), chitosan, and sodium fluoride. NSF was developed to provide the same effects as silver diamine fluoride (SDF) without causing tooth discoloration, a significant drawback of SDF (Santos et al. 2014). Previous studies comparing the antibacterial efficacy and cytotoxicity of NSF and SDF against *S. mutans* showed no significant difference in antibacterial efficacy, but NSF exhibited significantly lower cytotoxicity than SDF in MIC of *S. mutans* (Gultom et al. 2019; Targino et al. 2014). The AgNPs in NSF cause cell membrane damage through lipid peroxidation and oxidative damage to DNA and proteins, exhibiting high antibacterial activity against cariogenic bacteria like *S. mutans* and dental

biofilm (Pushpalatha et al. 2022). Chitosan, acting as a stabilizing agent in NSF, is a polycation that inhibits the cellular adherence process of *S. mutans*, thereby preventing dental biofilm formation (Ahmed et al. 2019). Additionally, chitosan can inhibit demineralization by preventing mineral release from enamel (Arnaud, de Barros Neto, and Diniz 2010). Fluoride prevents caries by adsorbing to the tooth surface, inhibiting mineral dissolution, promoting remineralization, and coating the surface with acid-resistant fluorapatite (ten Cate 1999). Therefore, developing a coating solution and method to apply NSF to orthodontic elastomerics would effectively prevent dental biofilm-related diseases in orthodontic patients.

Among the various oral bacteria, *S. mutans* is a primary contributor to cariogenic dental biofilm formation. *S. mutans* secretes glycosyltransferases (GTFs), which form glucans that establish an extracellular polysaccharide (EPS) matrix. The EPS-matured dental biofilm becomes acidogenic and aciduric, leading to dental caries (Bowen and Koo 2011). During orthodontic treatment, the levels of *S. mutans* in saliva and dental biofilm increase, raising the risk of caries due to the accumulation of cariogenic dental biofilm (Mummolo et al. 2020; Rosenbloom and Tinanoff 1991). Thus, an antimicrobial treatment strategy to reduce *S. mutans* in the oral cavity is necessary to prevent caries in orthodontic patients.

Additionally, the oral cavity harbors over 700 species of microorganisms, and dental biofilm is composed of multiple species (Aas et al. 2005). Multispecies dental biofilm increases antibacterial resistance through interactions between different species within the community (Hall and Mah 2017), Therefore, evaluating the anti-biofilm efficacy of newly

developed anti-caries agents against multispecies dental biofilm is crucial for assessing their clinical applicability.

The *in vitro* dental microcosm biofilm model, which uses human saliva as the inoculum, simulates the diversity and heterogeneity of microorganisms within actual dental biofilm, replicating the human oral environment (Wong and Sissions 2001). Therefore, this study aimed to develop NSF coated orthodontic elastomerics (nano silver fluoride sustained-release orthodontic elastomerics; NSF-RE) by exploring the optimal coating solution combination. The antibacterial and demineralization-inhibiting effects of NSF-RE were comprehensively evaluated using the dental microcosm biofilm model to explore their clinical applicability.

The detailed objectives of this study are as follows. The first study aimed to evaluate the optimal coating solution composition by comparing and analyzing the release amount of AgNPs, fluoride, and tensile strength among elastomerics coated with different solution compositions. The second study aimed to evaluate the antibacterial persistence effect of NSF-RE against *S. mutans* and the anti-biofilm effect against *S. mutans* biofilm. The third study aimed to comprehensively evaluate the anti-biofilm and demineralization-inhibiting effects of NSF-RE using a multispecies dental microcosm biofilm model.

The null hypotheses of this study were as follows. In the first study, there were no differences in AgNPs release, fluoride release, and tensile strength among elastomerics coated with different solution compositions. In the second study, the antibacterial

persistence and anti-biofilm effect of NSF-RE against *S. mutans* would not be different from that of the negative control. In the third study, the anti-biofilm and demineralization-inhibiting effects of NSF-RE against dental microcosm biofilms would not be different from those of the negative control.

2. Materials and Methods

In the first study, the presence of NSF was confirmed using a UV-Vis spectrophotometer and transmission electron microscopy (TEM). The release of AgNPs and fluoride from NSF-RE for 7 days was quantified using a UV-Vis spectrophotometer and a fluoride electrode, respectively. while the mechanical properties were assessed through tensile strength. In the second study, the antimicrobial persistence of NSF-RE against *S. mutans* was evaluated using an agar diffusion test, and the anti-biofilm effect was assessed through colony-forming units (CFUs) and confocal laser scanning microscopy (CLSM). The third study evaluated the anti-biofilm effect of NSF-RE using an *in vitro* microcosm biofilm model, assessing biofilm maturity through red/green ratio (R/G ratio), CFUs, CLSM, and microbial composition. The demineralization-inhibiting effect was evaluated by enamel fluorescence loss (ΔF, ΔF_{max}). The effective distance of the substances released from the elastomerics was evaluated by $\Delta\Delta F$ (Fig. 1).

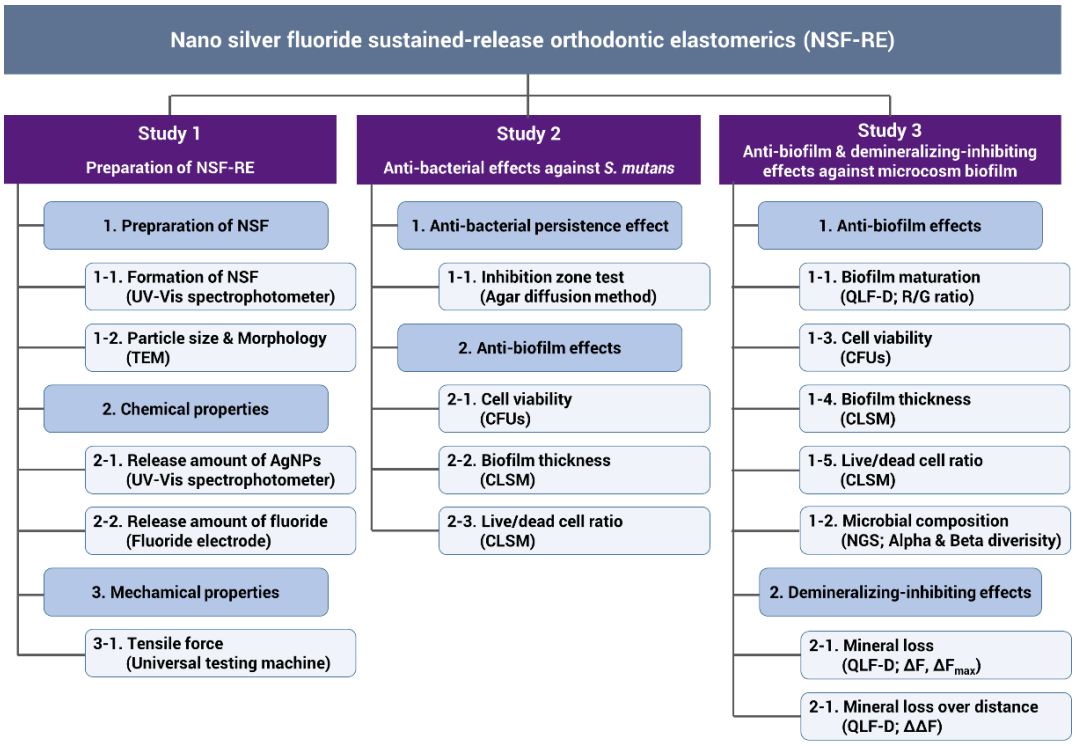

Figure 1. Flow diagram of the assessment of nano silver fluoride sustained-release elastomerics development and evaluation.

2.1 Chemical and mechanical properties of nano silver fluoride-sustained release orthodontic elastomerics (Study I)

2.1.1 Preparation of nano silver fluoride

NSF used in this study was prepared based on previous research (Targino et al. 2014). To produce the NSF colloidal solution, silver nitrate ($AgNO_3$) was reduced using sodium borohydride ($NaBH_4$), and the compound was stabilized with chitosan biopolymer. In detail, chitosan (2.5 mg/mL) was dissolved in 1% acetic acid and stirred overnight with a magnetic stirrer. The chitosan mixture was then filtered using a vacuum filter and transferred to an ice-cold bath. With vigorous stirring, $AgNO_3$ (0.11 mol/L) was added to the mixture, followed by the dropwise addition of prepared $NaBH_4$ (0.8 mol/L). The mixture was removed from the ice-cold bath, and sodium fluoride (10,147 ppm) was added and stirred overnight to produce NSF with concentrations of 399.33 μg/mL AgNPs, 2,334 μg/mL chitosan, and 10,147 μg/mL fluoride.

2.1.2 Preparation of nano silver fluoride sustained-release orthodontic elastomerics

To coat the elastomerics with NSF, four experimental coating solutions were prepared by mixing ethyl cellulose (EC; N100, Sigma-Aldrich, MO, USA) and polyethylene glycol 6000 (PEG; Duksan, Ansan, Korea) in different compositions with dichloromethane (DCM; JUNSEI, Tokyo, Japan) containing NSF. The prepared coating solutions exhibited concentrations of 92 μg/mL AgNPs, 537 μg/mL chitosan, and 2,334 μg/mL fluoride. Four

experimental groups were denoted: a coating solution without EC and PEG (NSF), a solution with EC only (NSF-E), a solution with EC and PEG at a 4:1 ratio (NSF-EP1), and a solution with EC and PEG at a 2:1 ratio (NSF-EP2) (Table 1). Orthodontic elastomerics (TP Orthodontics, IN, USA) of 1/8 inch, 0.005g, forces of 3.2 oz (20 mm) and 3.7 oz (30 mm) were washed with sterilized distilled water (DW) and dried in a 60°C oven for 1 h. The elastomerics were then dipped in each coating solution using the dip coating method. The elastomerics were dipped once in the prepared coating solution, and dried at room temperature for 1 h, and the process was repeated twice to produce the coated elastomerics. The three groups of elastomerics coated with solutions containing EC (NSF-E, NSF-EP1, NSF-EP2) were denoted as NSF-RE (Fig. 2). Uncoated and dried elastomerics were denoted as the negative control.

Table 1. Chemical compositions of the coating solutions for making orthodontic elastomerics.

Groups	Drug (mL)	Polymer (mg)	Plasticizer (mg)	Solvent (mL)
	Nano silver fluoride	Ethyl cellulose	Polyethylene glycol 6000	Dichloromethane
Control	—	—	—	—
NSF	0.3	—	—	1
NSF-E	0.3	20	—	1
NSF-EP1	0.3	20	5	1
NSF-EP2	0.3	20	10	1

NSF, Nano silver fluoride; E, ethyl cellulose, EP; ethyl cellulose with polyethylene glycol 6000.

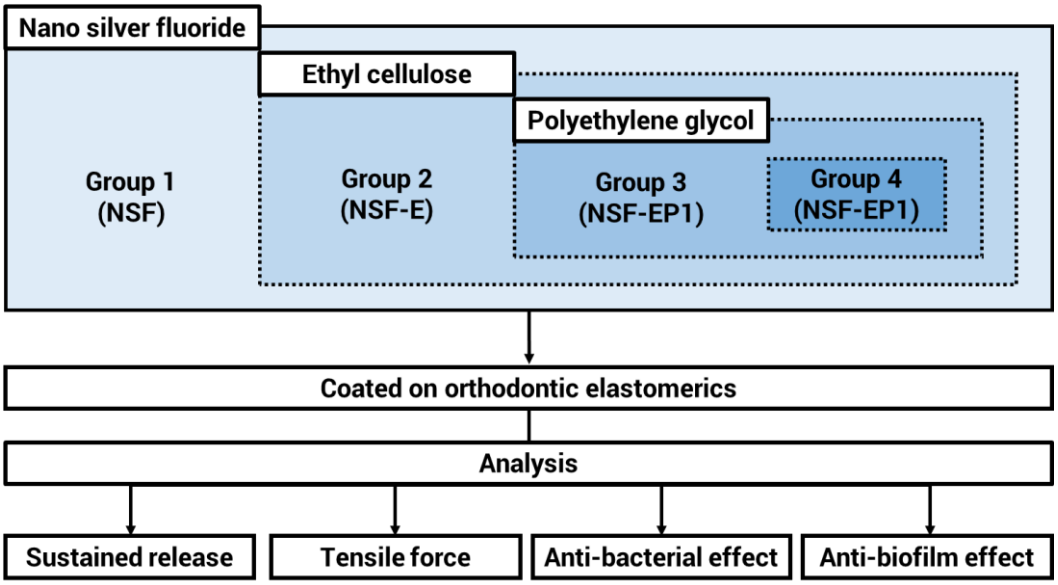

Figure 2. Flow diagram of preparing and evaluating nano silver fluoride sustained-release orthodontic elastomerics in studies 1 and 2.

2.1.3 Sustained release effects of silver nanoparticles and fluoride from the coated elastomerics

To evaluate the sustained release of AgNPs and fluoride from the coated elastomerics, 20 coated elastomerics were fixed to orthodontic ligature wires and immersed in 4 ml of DW in 8 ml vials, which were kept in a 37°C incubator. The DW was replaced at intervals. During the first 24 h, DW was replaced at 1, 4, 8, 12, and 24 h, and subsequently every 24 h up to 168 h. The concentrations of AgNPs and fluoride in the remained DW were measured to evaluate the cumulative release from the coated elastomerics. This procedure was repeated three times.

To evaluate the cumulative release of AgNPs from the coated elastomericss, standard AgNPs of varying concentrations were prepared, and their absorbance was measured using a UV-Vis spectrophotometer to create a calibration curve. The absorbance of DW samples at each time point was then measured and converted to AgNP concentrations.

For evaluating the cumulative release of fluoride from the coated elastomerics, an Orion ionplus Fluoride Electrode 9609 (Orion Research, MA, USA) and a pH/ISE meter were used. Standard fluoride solutions of different concentrations were prepared, and TISAB II was added in a 1:1 (V/V) ratio to create a calibration curve. The fluoride concentration in the DW samples at each time point was then measured.

2.1.4 Tensile force of the coated elastomerics

To ensure that the elastomerics coated with each coating solution could be stably attached to orthodontic brackets, tensile strength was measured using a universal testing machine (Instron 3366, MA, USA). The tensile force (N) required to stretch each elastomerics at 2 mm/min or 3 mm/min was measured for a total of 10 elastomerics per group.

2.2 Antibacterial activity of NSF-RE on *S. mutans* (Study II)

2.2.1 Bacterial strain

S. mutans ATCC 25175 (Korea Research Institute of Bioscience and Biotechnology, Seoul, Korea) was inoculated in Brain Heart Infusion (BHI) broth and cultured at 37°C with 10% CO_2 for 24 h. The culture was mixed with 80% glycerin at a 1:1 ratio to prepare a stock. The stock was stored at −80°C, and the same stock was used for each experiment.

2.2.2 Antimicrobial persistence effects of the coated elastomerics against *Streptococcus mutans*

The antibacterial effect of the coated elastomerics on *S. mutans* was evaluated using the agar diffusion test as described by a previous study (Jeon et al. 2017). Pre-incubated 10^7 CFU/ml *S. mutans* 100 μL in BHI broth was inoculated and spread on BHI agar. Four coated elastomerics were placed on the surface of the inoculated BHI agar and incubated at 37°C with 10% CO_2 for 24 h. The coated elastomerics were then carefully transferred to fresh BHI agar inoculated with *S. mutans*. This process was repeated for 7 days. After 7 days, the BHI agar with inhibition zones was photographed with a digital camera, and the diameter of the inhibition zones around each of the coated elastomerics was measured using the ImageJ analysis program (ImageJ with 64-bit Java 1.8.0_112 National Institute of Health, USA). This process was repeated three times.

2.2.3 *S. mutans* biofilm formation

Hydroxyapatite (HA) discs with elastomerics attached to the center were prepared using the method described by a previous study (Choi et al. 2022). A sterilized microbrush tip (cut to 3 mm; TPC, CA, USA) was fixed on the sterilized HA disc surface using the composite resin (DenFil Flow, VERICOM, Chuncheon, Korea) to complete the specimens. A modified version of the *S. mutans* biofilm model described by a previous study was used in this study (Guggenheim et al. 2004). Each specimen was immersed in 1.5 ml of artificial saliva (pH 6.8, containing 2.2 g/L gastric mucin, 0.381 g/L NaCl, 0.213 g/L $CaCl_2 \cdot 2H_2O$, 0.738 g/L KH_2PO_4, and 1.11 g/L KCl) in a 24-well plate and incubated at 37°C with 10% CO_2 for 4 h to form an acquired pellicle. The specimens were then transferred to a mixture of 800 μl artificial saliva, 800 μl Todd Hewitt yeast extract broth, and 200 μl *S. mutans* adjusted to 10^7 CFU/ml and incubated at 37°C with 10% CO_2. After 16 h of biofilm formation, the specimens were rinsed three times with DW to remove planktonic bacteria. The specimens were then transferred to a fresh artificial saliva-broth mixture to promote biofilm regrowth. This process was repeated after 40 h, and the biofilm was cultured for a total of 64 h (Fig. 3).

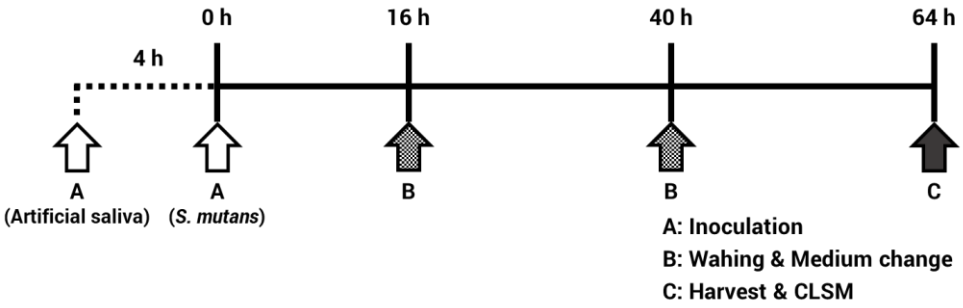

Figure 3. Flow diagram of the experimental procedures for evaluating the anti-biofilm effect of the coated elastomerics against *S. mutans* biofilm.

2.2.4 Cell viability in *S. mutans* biofilm

To evaluate the anti-biofilm effect of the coated elastomerics, CFUs of *S. mutans* were counted from the biofilm on 9 specimens per group. The specimens with the 64 h matured biofilm were rinsed three times with 1.5 ml of DW to remove loosely attached planktonic bacteria and transferred to a 15 ml conical tube, containing 1 ml of DW. The samples were then vortexed for 1 min and sonicated at 40 kHz for 1 min. The bacterial suspension was serially diluted, plated on BHI agar, and incubated at 37°C with 10% CO_2 for 48 h, followed by CFU counting.

2.2.5 CLSM analysis of *S. mutans* biofilm

For quantitative analysis of the biofilm thickness and live/dead cell ratio of *S. mutans*, confocal laser scanning microscopy (CLSM; LSM880, Carl Zeiss, Jena, Germany) was used. The 64 h matured biofilm was stained using the LIVE/DEAD BacLight Bacterial Viability Kit (Molecular Probes, Eugene, OR, USA). Live bacteria were stained with SYTO9, exhibiting green fluorescence, and dead bacteria were stained with propidium iodide, exhibiting red fluorescence. Five random locations on each specimen were imaged as Z-stacks, and two specimens per group were analyzed. The acquired images were processed using the COMSTAT plug-in (Technical University of Denmark, Kongens Lyngby, Denmark) in ImageJ to calculate the biofilm thickness and live/dead cell ratio.

2.3. Anti-biofilm and demineralization-inhibiting effects of NSF-RE on dental microcosm biofilms (Study III)

2.3.1 Enamel specimen preparation

Bovine incisors without cracks or white spots were sectioned (8 mm in diameter and 3 mm thick) and polished with 600, 800, 1,000, and 1,200 grit sandpapers. To evaluate the mineral loss of enamel beneath the biofilm by fluorescence loss (ΔF, ΔF_{max}), half of the prepared enamel specimens were covered with acid-resistant nail varnish (Nail Top Coat, Innisfree, Seoul, Korea) (Kang and Kim 2021). After the nail varnish dried, the specimens

were embedded in sterile acrylic molds 1 mm below the surface to create enamel specimens. The specimens were sterilized using an autoclave, and a 3 mm sterilized microbrush tip (TPC, CA, USA) was fixed in the center with light-cured acrylic resin (Ortho-Jet Powder, Jet Liquid, IL, USA). In Study 3, two experimental groups were denoted: one with a solution containing only EC (NSF-E) and the other with a solution containing EC and PEG in a 2:1 ratio (NSF-EP). All elastomerics coated with the prepared solutions were named NSF-RE (Fig. 4). Three elastomerics from each group were attached to the tip, completing the specimens for this experiment (Fig. 5)

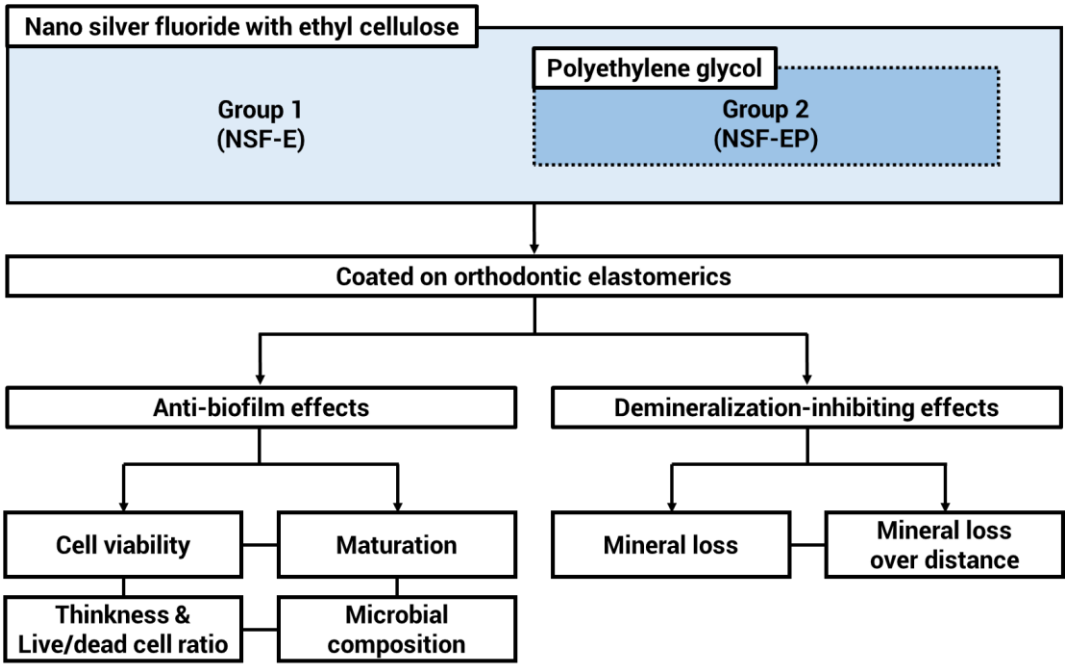

Figure 4. Flow diagram of preparing and evaluating nano silver fluoride sustained-release orthodontic elastomerics in study 3.

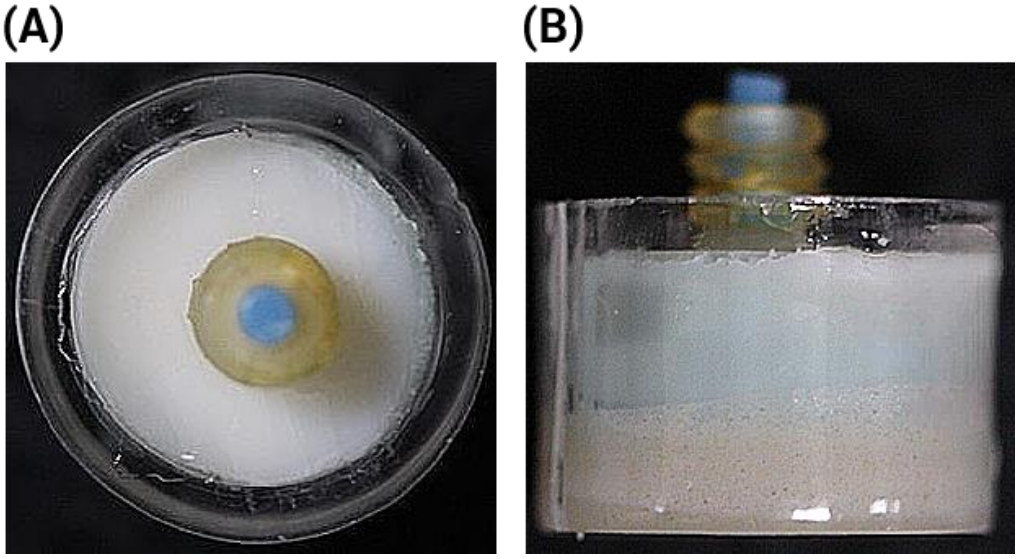

Figure 5. Images of enamel specimens representing the oral cavity of orthodontic patients. (A) Top view, (B) Side view.

2.3.2 Formation of dental microcosm biofilms

Microcosm biofilms were formed using the model developed by a previous study (Lee et al. 2018). Stimulated saliva from healthy adult males without caries or periodontal disease and who had not performed any oral hygiene for 24 h was used as the inoculum. Ethical approval for saliva collection was granted by the Ethics Committee of Yonsei Dental Hospital (IRB No. 2-2023-0054) and conducted according to the guidelines of the Helsinki Declaration. Collected saliva was filtered through sterilized glass wool to remove debris, mixed with sterilized glycerol, and prepared as a stock solution of 30% saliva and 70% glycerol. The stock solution was stored at −80°C and used consistently for each experiment. Each specimen was inoculated with 1.5 ml of saliva in a 24-well plate and incubated at 37°C with 10% CO_2 for 4 h to form an acquired pellicle. After 4 h, the saliva was carefully aspirated from the wells, and 1.5 ml of basal medium mucin with 0.3% sucrose was added. The 24-well plates containing the specimens were incubated at 37°C in an anaerobic environment (80% N_2, 10% CO_2, and 10% H_2). Specimens were rinsed three times with cysteine peptone water (CPW) every 24 h and transferred to new wells containing 1.5 ml of fresh medium to induce biofilm regrowth for 7 days (Fig. 6).

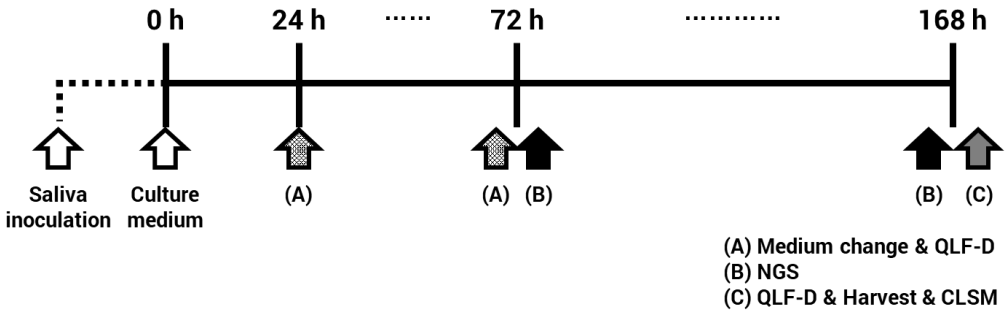

Figure 6. Flow diagram of the experimental procedures for evaluating the anti-biofilm effect of the coated elastomerics against dental microcosm biofilms.

2.3.3 Biofluorescence detection of dental microcosm biofilms and image analysis

To assess biofilm maturation using changes in biofluorescence, images were captured with a quantitative light-induced fluorescence-digital (QLF-D) Biluminator device (Inspektor Research Systems, Amsterdam, The Netherlands). All specimens were imaged under conditions of 1/45 s shutter speed, 7.2 aperture, and ISO speed of 1,600 at 24 h intervals for 7 days. The red fluorescence intensity of the biofilm was compared using the

ImageJ analysis program (ImageJ with 64-bit Java 1.8.0_112, National Institute of Health, USA). Areas of interest (AOI) were set to exclude the elastomerics in the center and only cover the biofilm on the specimen surface to calculate the R/G ratio.

2.3.4 Cell viability in dental microcosm biofilms

To evaluate the inhibitory effects of NSF-Ef and NSF-EP on dental microcosm biofilm formation, total and aciduric bacteria CFUs were measured after 7 days of maturation. Each specimen with a 7-day matured biofilm was rinsed three times with 1.5 ml of CPW to remove loosely attached planktonic bacteria, then transferred to a 15 ml conical tube containing 2 ml of CPW. The samples were vortexed for 1 min and sonicated at 40 kHz for 1 min. The bacterial suspension was serially diluted and spread on 5% tryptic soy broth blood agar plates (for total bacteria) and brain heart infusion agar plates adjusted to pH 4.8 (for aciduric bacteria). The plates were incubated anaerobically at 37°C for 72 h, and CFUs were counted to evaluate biofilm cell viability.

2.3.5 CLSM analysis of dental microcosm biofilms

The 7-day matured biofilm was stained using the LIVE/DEAD BacLight Bacterial Viability Kit. Each specimen was imaged at five randomly selected locations using CLSM (LSM900, Carl Zeiss, Jena, Germany) as Z-stacks, with two specimens per group imaged. The acquired images were analyzed using the COMSTAT plug-in in ImageJ to calculate biofilm thickness and live/dead cell ratio.

2.3.6 Microbiome taxanomic profiling of dental microcosm biofilms

Total DNA was isolated using the Maxwell RSC PureFood GMO and Authentication Kit (Promega) following the manufacturer's guidelines. PCR amplification was conducted with fusion primers targeting the V3 to V4 regions of the 16S rRNA gene from the extracted DNA. For bacterial amplification, the fusion primers used were 341F (5'-AATGATACGGCGACCACCGAGATCTACAC-XXXXXXXX-TCGTCGGCAGCGTC-AGATGTGTATAAGAGACAG-CCTACGGGNGGCWGCAG-3'; target region primer sequence underlined) and 805R (5'-CAAGCAGAAGACGGCATACGAGAT-XXXXXXXX-GTCTCGTGGGCTCGG-AGATGTGTATAAGAGACAG-GACTACHVGGGTATCTAATCC-3'). The fusion primers comprised P5 (P7) graft binding, i5 (i7) index, Nextera consensus, sequencing adaptor, and target region sequence. The amplification protocol included initial denaturation at 95°C for 3 minutes, 25 cycles of denaturation at 95°C for 30 seconds, primer annealing at 55°C for 30 seconds, and extension at 72°C for 30 seconds, followed by a final elongation at 72°C for 5 minutes. PCR products were verified using 1% agarose gel electrophoresis and visualized with a Gel Doc system (BioRad, Hercules, CA, USA). The amplified products were purified using CleanPCR (CleanNA). Equal concentrations of purified products were pooled, and short fragments (non-target products) were removed with CleanPCR (CleanNA). The quality and product size were evaluated on a Bioanalyzer 2100 (Agilent, Palo Alto, CA, USA) using a DNA 7500 chip. The mixed amplicons were sequenced at CJ Bioscience, Inc. (Seoul, Korea), using the Illumina MiSeq Sequencing system (Illumina, USA) according to the

manufacturer's protocol.

The processing of raw reads began with a quality check and filtering of low-quality reads (<Q25) using Trimmomatic ver. 0.32 (Bolger, Lohse, and Usadel 2014). After passing quality control, paired-end sequences were merged using the fastq_mergepairs command of VSEARCH version 2.13.4 (Rognes et al. 2016) with default parameters. Primers were trimmed using the alignment algorithm of Myers & Miller (Myers and Miller 1988) at a similarity cutoff of 0.8. Non-specific amplicons, not encoding 16S rRNA, were identified using nhmmer (Wheeler and Eddy 2013) in the HMMER software package ver. 3.2.1 with hmm profiles. Unique reads were extracted, and redundant reads were clustered with the unique reads using the derep_fulllength command of VSEARCH (Rognes et al. 2016). The EzBioCloud 16S rRNA database (Yoon et al. 2017) was utilized for taxonomic assignment via the usearch_global command of VSEARCH2, followed by precise pairwise alignment (Myers and Miller 1988). Chimeric reads were filtered by reference-based chimera detection using the UCHIME algorithm (Edgar et al. 2011) and the non-chimeric 16S rRNA database from EzBioCloud. Reads not identified to the species level (<97% similarity) in the EzBioCloud database were clustered de novo using the cluster_fast command2 to generate additional OTUs. OTUs with single reads (singletons) were excluded from further analysis.

2.3.7 Fluorescence imaging of enamel and image analysis

After 7 days of biofilm maturation, the biofilm on the specimen surface was removed to

observe the enamel fluorescence loss. The nail varnish on the enamel surface was removed using acetone (Duksan, Ansan, Korea), and the specimen surface was completely dried with an air-dryer for 15 s. Fluorescence images of the enamel surface were obtained using QLF-D with a shutter speed of 1/45 s, aperture of 7.2, and ISO speed of 1,600. The captured images were analyzed using the QA2 program (Version 1.24, Inspektor Research System BV, Amsterdam, The Netherlands) with the White Spot Patch function to calculate the fluorescence loss (ΔF; %) and maximum fluorescence loss (ΔF_{max}; %) (Fig. 7, A). To evaluate the effective distance of AgNPs and fluoride released from the elastomerics, ΔF (%) was calculated at three points at 1 mm intervals starting from the point of demineralization initiation (Fig. 7, B). The difference in ΔF (%) between the experimental and control groups was calculated to obtain ΔΔF for NSF-E and NSF-EP.

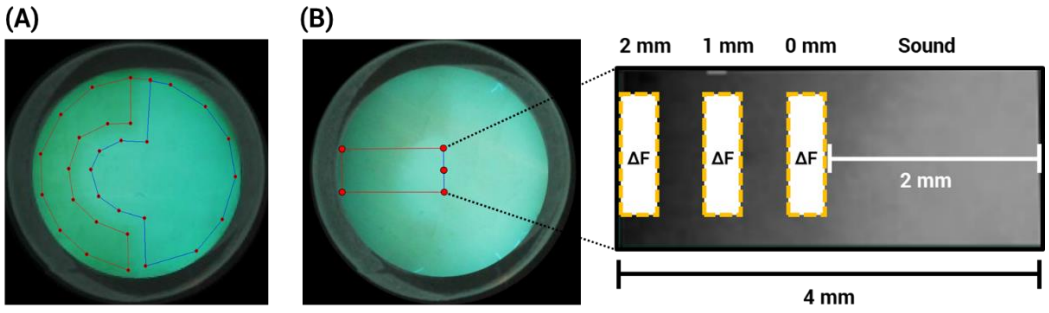

Figure 7. Area of interest (AOI) of QLF images using QA2J software. (A) AOI of the demineralized area of the specimen, (B) AOI at varying distances from the sound area.

2.3.8 Statistical analysis

Statistical analyses were performed using the Statistical Package for the Social Sciences (SPSS) version 27.0 (SPSS Inc, Chicago, IL, USA) with a significance level of 0.05. A sample size of at least 9 per group was used for all evaluations. Parametric statistical methods were applied for normally distributed data, and non-parametric methods were used for non-normally distributed data. A One-way ANOVA with Tukey's post hoc test was conducted to examine differences in AgNPs and fluoride release, *S. mutans* biofilm cell viability, and all evaluation parameters in microcosm biofilms between groups. The Kruskal-Wallis test followed by the Mann-Whitney U test was used to analyze differences in tensile strength, inhibition zones, and *S. mutans* biofilm thickness and live/dead cell ratios between groups. Microbial diversity calculations were performed using the EzBioCloud 16S-based MTP bioinformatics cloud platform from CJ Bioscience, Inc. (Seoul, Korea). The alpha diversity index (Shannon) and beta diversity distances using Bray-Curtis were calculated to visualize differences between samples.

3. Results

3.1 Chemical and mechanical properties of nano silver fluoride-sustained release orthodontic elastomerics (Study I)

3.1.1 Characterization of the nano silver fluoride

The NSF fabricated in this study was evaluated using UV-Vis spectroscopy (JASCO V-650 Spectrophotometer, Tokyo, Japan). The results showed a maximum peak at 397 nm, which is consistent with the spectrum of chitosan-stabilized AgNPs (Fig. 8, A). The morphology and dispersion of the NSF particles were assessed using TEM, revealing spherical particles with an average diameter of 9.56 ± 3.26 nm and monodisperse characteristics (Fig. 8, B).

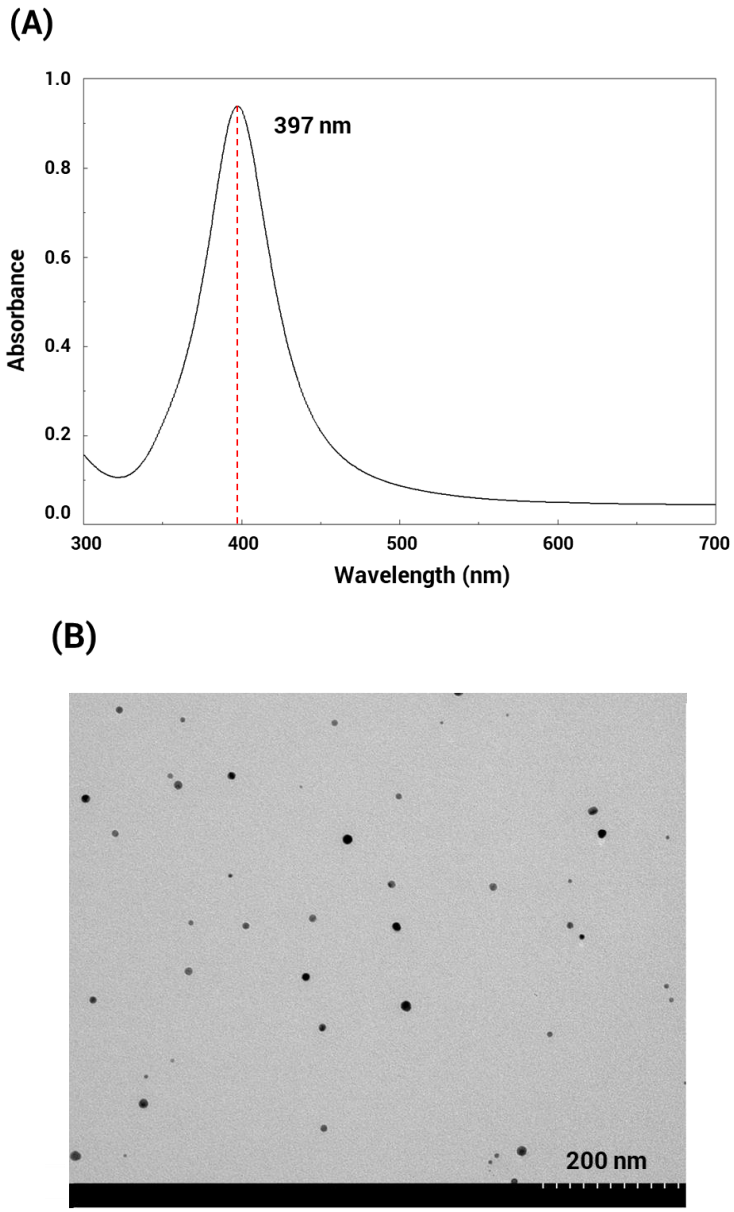

Figure 8. Nano silver fluoride (NSF) characterization. (A) UV-Vis spectra of NSF, (B) Transmission electron microscopy image of NSF.

3.1.2 Silver nanoparticles release from the coated elastomerics

The NSF-RE groups containing EC continuously released AgNPs for 7 days, whereas NSF without EC ceased releasing AgNPs within 48 h (Fig. 9). Comparing the amount of AgNPs released across different groups, the amount of AgNPs released increased until day 7. The cumulative amount of AgNPs released for 7 days was 16.9 ppm for NSF, 44.2 ppm for NSF-E, 43.3 ppm for NSF-EP1, and 63.8 ppm for NSF-EP2, with NSF-EP2 showing significantly higher cumulative release than other groups ($P < 0.001$). Within the first 12 h, the release amounts were 80% for NSF, 58% for NSF-E, 76% for NSF-EP1, and 85% for NSF-EP2, with NSF-EP2 exhibiting significantly faster release ($P < 0.001$). From 12 h to 7 days, the release amounts were 3.4 ppm for NSF, 18.7 ppm for NSF-E, 10.2 ppm for NSF-EP1, and 9.4 ppm for NSF-EP2, with NSF-E releasing 5.5 times more AgNPs than NSF (Fig. 9).

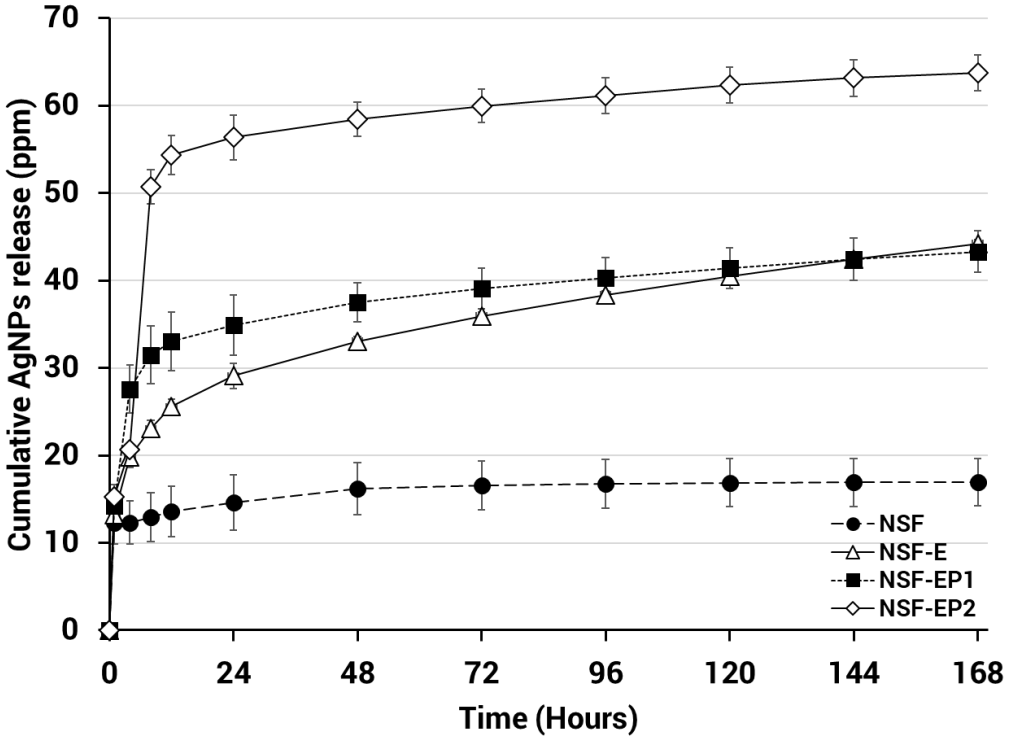

Figure 9. Cumulative mass of AgNPs released from the coated elastomerics (n = 20).

3.1.3 Fluoride release from the coated elastomerics

Evaluation of the fluoride release duration from the coated elastomerics showed that the NSF-RE groups containing EC continuously released fluoride for 7 days. Conversely, NSF group ceased releasing fluoride within 12 h (Fig. 10). The amount of fluoride released increased until day 7 in all groups. The cumulative amount of fluoride released for 7 days was 5.6 ppm for NSF, 7.2 ppm for NSF-E, 8.4 ppm for NSF-EP1, and 9.2 ppm for NSF-EP2, with NSF-EP2 showing the highest release. NSF-EP2 released significantly more fluoride than NSF and NSF-E by factors of 1.64 and 1.28, respectively ($P < 0.001$ and $P = 0.001$, respectively). Within the first 12 h, the release amounts were 98% for NSF, 83% for NSF-E, 65% for NSF-EP1, and 79% for NSF-EP2, with NSF exhibiting significantly higher release rates than the other groups ($P < 0.001$). However, from 12 h to 7 days, the release amounts were 0.1 ppm for NSF, 1.2 ppm for NSF-E, 3.0 ppm for NSF-EP1, and 2.0 ppm for NSF-EP2, with NSF-EP1 releasing the most (Fig. 10). The NSF-EP2, which contained EC and PEG in a 2:1 ratio, released the most AgNPs and fluoride for 7 days compared to the other groups.

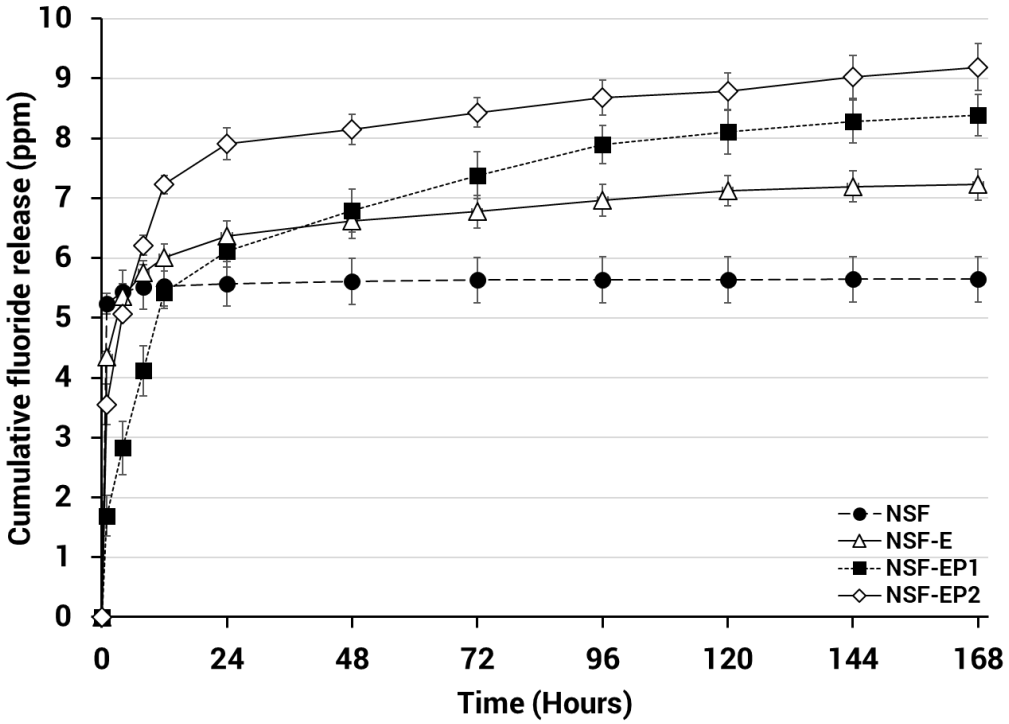

Figure 10. Cumulative mass of fluoride released from the coated elastomerics (n = 20).

3.1.4 Tensile force of the coated elasteomrics

To evaluate if the antimicrobial-coated orthodontic elastomerics with NSF and EC could be stably attached to orthodontic brackets, a tensile strength evaluation was conducted. The results showed that the tensile strength increased with the elongation of the elastomerics; however, there were no statistically significant differences in tensile strength between the groups based on the presence or absence of coating and the type of coating solution (Table 2).

Table 2. Tensile force of the coated elastomerics (Unit: N).

Groups	2 mm tensile strength	3 mm tensile strength
Control	4.53 (0.64)[a]	5.55 (0.50)[a]
NSF	4.40 (0.50)[a]	5.43 (0.43)[a]
NSF-E	4.21 (0.46)[a]	5.26 (0.47)[a]
NSF-EP1	4.65 (0.70)[a]	5.57 (0.67)[a]
NSF-EP2	4.36 (0.31)[a]	5.28 (0.34)[a]

Data represent mean (standard deviation) values. NSF, nano silver fluoride; E, ethyl cellulose, EP; ethyl cellulose with polyethylene glycol 6000. Different small letters within the same column indicate significant differences between groups by Kruskal-Wallis test with post hoc Mann-Whitney U test ($P < 0.05$, $n = 10$).

3.2 Antibacterial activity of NSF-RE on *S. mutans* (Study II)

3.2.1 Antimicrobial persistence effect on *S. mutans*

To evaluate the antimicrobial persistence of the coated elastomerics, the inhibition zone on the surface of BHI agar inoculated with *S. mutans* was measured (Fig. 11, A). On day 7, the inhibition zone for NSF-EP2 (8.51 mm) was significantly larger than that for NSF (3.22 mm) and NSF-E (6.49 mm), by factors of 2.64 and 1.31, respectively ($P < 0.001$ and $P < 0.001$, respectively). However, there was no significant difference compared to NSF-EP1 (7.28 mm). Groups containing EC (NSF-E, NSF-EP1, NSF-EP2) exhibited significantly larger inhibition zones, 2.31 times greater than those without EC (NSF) ($P < 0.001$, Fig. 11, B).

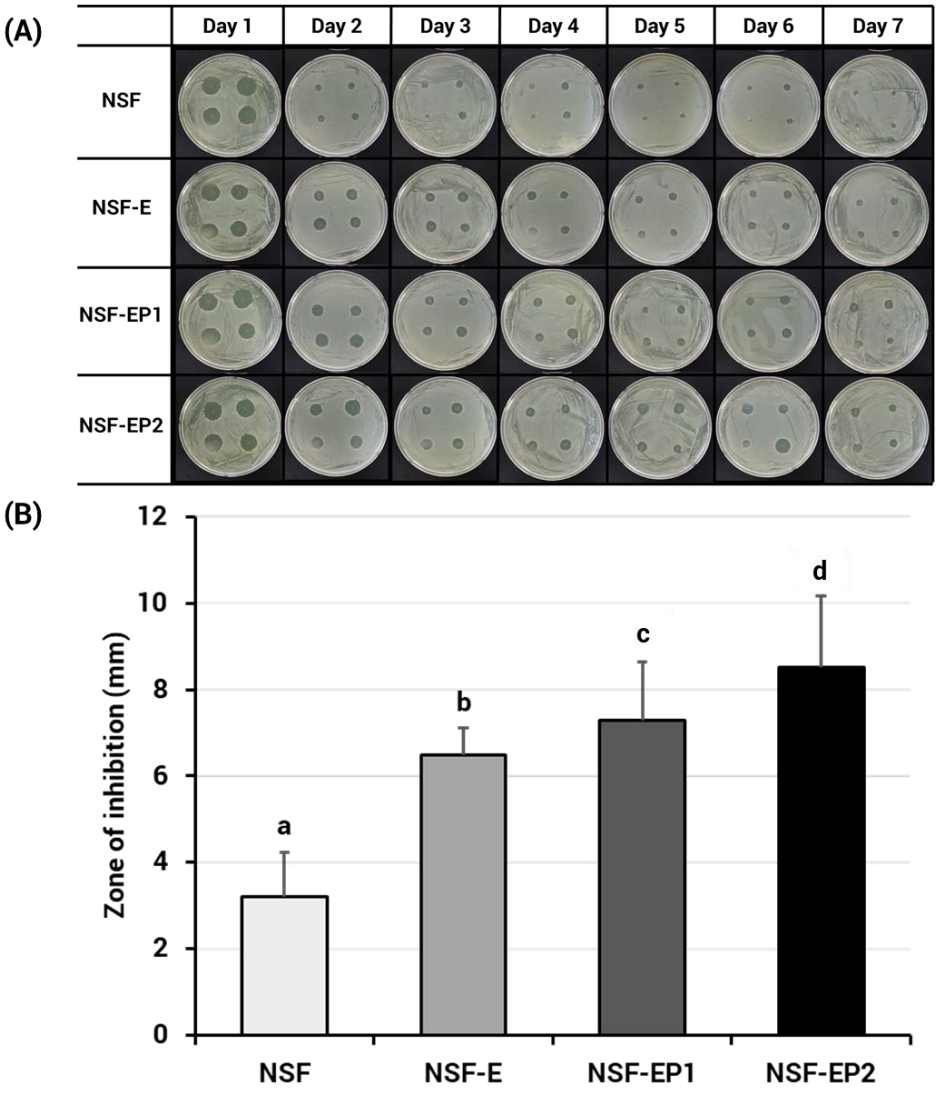

Figure 11. Antimicrobial persistence effect for different coated elastomerics groups against *S. mutans*. (A) Inhibition zone for 7 days, (B) Diameter of the inhibition zone (mm) on day 7. Different small letters (a, b, c, d) indicate significant differences between groups by Kruskal-Wallis test with post hoc Mann-Whitney U test, $P < 0.05$; $n = 12$.

3.2.2 Cell viability of *S. mutans* biofilm

The evaluation of cell viability in 64 h mature *S. mutans* biofilm showed reductions of 2% for NSF, 43% for NSF-E, 50% for NSF-EP1, and 57% for NSF-EP2 compared to the control group. The CFUs in EC-containing groups (NSF-RE) were significantly lower than those in the control ($P < 0.001$). Among NSF-RE groups, NSF-EP2 exhibited 24% significantly lower CFUs compared to NSF-E ($P < 0.001$, Fig. 12).

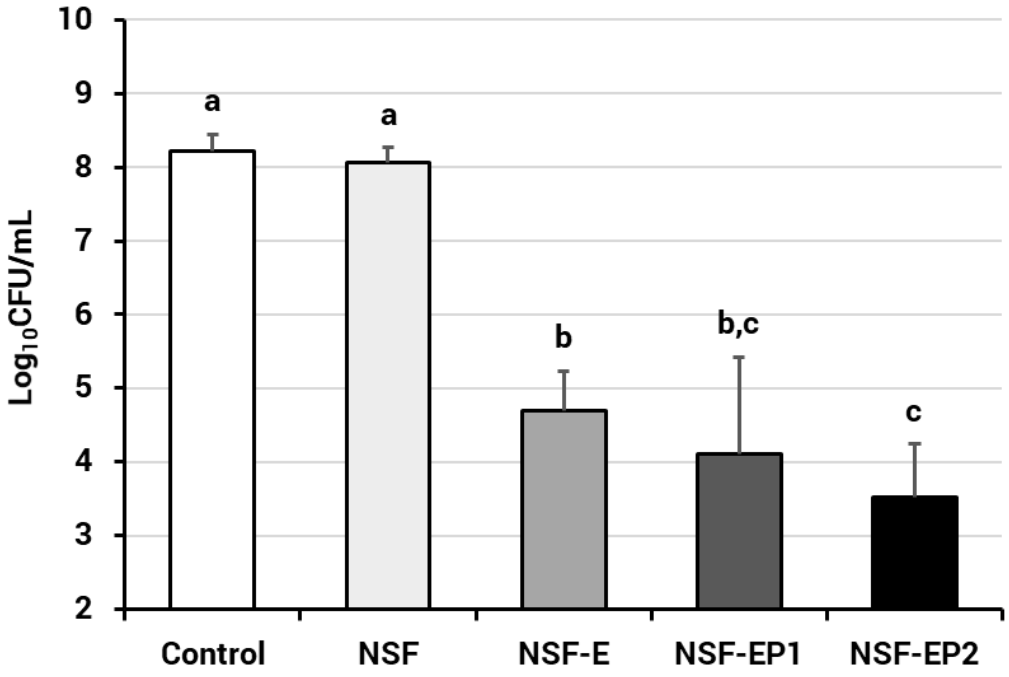

Figure 12. Viable bacteria in 64 h mature *S. mutans* biofilm grown in the different groups. Different small letters (a, b, c) indicate significant differences between groups by ANOVA test with post hoc Tukey HSD test, $P < 0.05$, $n = 9$.

3.2.3 Thickness and live/dead cell ratio of *S. mutans* biofilm

The thickness and live/dead cell ratio of the 64 h mature biofilm were evaluated using CLSM. Compared to the control, all EC-containing NSF-RE groups showed significant reductions. The specimens with EC-coated elastomerics had less *S. mutans* biofilm formation and a higher proportion of dead cells compared to live cells, as confirmed by CLSM images (Fig. 13). Specifically, NSF-EP2 showed an approximately 83% significant reduction in biofilm thickness ($P < 0.001$) and a 96% significant reduction in the live/dead cell ratio ($P < 0.001$, Table 3).

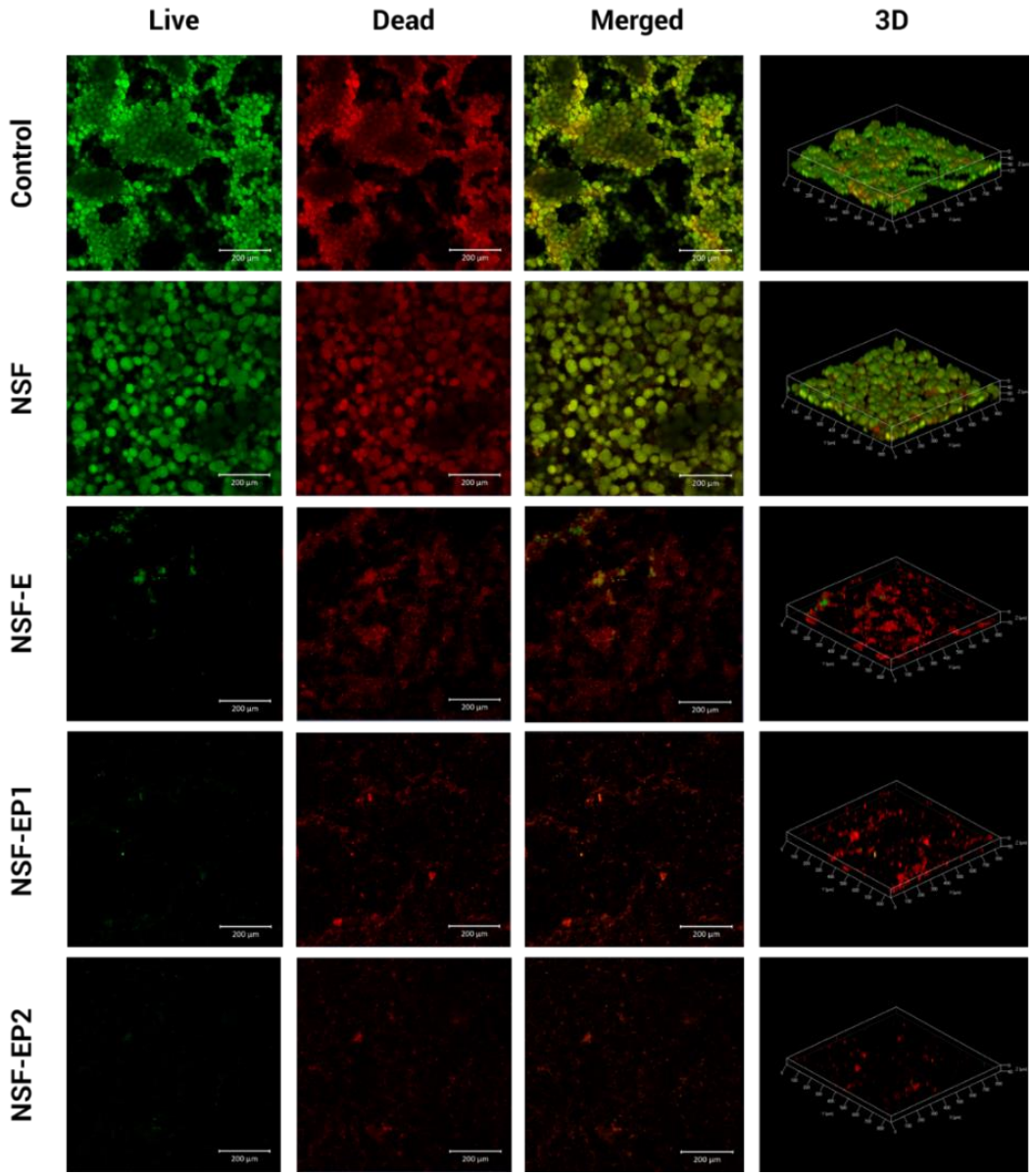

Figure 13. Confocal laser scanning microscopy images showing live/dead cells in stained *S. mutans* biofilms after 64 h, by group.

Table 3. Quantitative analysis of thickness and live/dead cell ratio of *S. mutans* biofilm using COMSTAT (n = 10).

Groups	Thickness (μm)	Live/dead cell ratio
Control	127.86 (14.55)[a]	1.08 (0.34)[a]
NSF	102.37 (36.95)[a]	1.05 (0.29)[a]
NSF-E	42.81 (9.92)[b]	0.14 (0.10)[b]
NSF-EP1	32.79 (8.19)[c]	0.07 (0.04)[b]
NSF-EP2	21.43 (3.24)[d]	0.04 (0.02)[b]

Data represent mean (standard deviation) values. NSF, nano silver fluoride; E, ethyl cellulose, EP; ethyl cellulose with polyethylene glycol 6000. Different small letters (a, b, c, d) within the same column indicate significant differences between groups by Kruskal-Wallis test with post hoc Mann-Whitney U test ($P < 0.05$).

3.3 Antimicobial activity of NSF-RE on dental microcosm biofilms (Study III)

3.3.1 Red fluorescence of dental microcosm biofilms

The R/G ratio was observed for 7 days of biofilm maturation after saliva inoculation, showing a gradual increase in all groups (Figs. 14, 15). After 3 days of biofilm formation, the R/G ratio in NSF-E and NSF-EP groups was significantly lower than in the control group ($P = 0.012$ and $P = 0.013$, respectively). On day 7 of biofilm formation, the R/G ratio in control was significantly higher than in NSF-E and NSF-EP by 27% and 34%, respectively ($P = 0.029$ and $P = 0.004$, respectively).

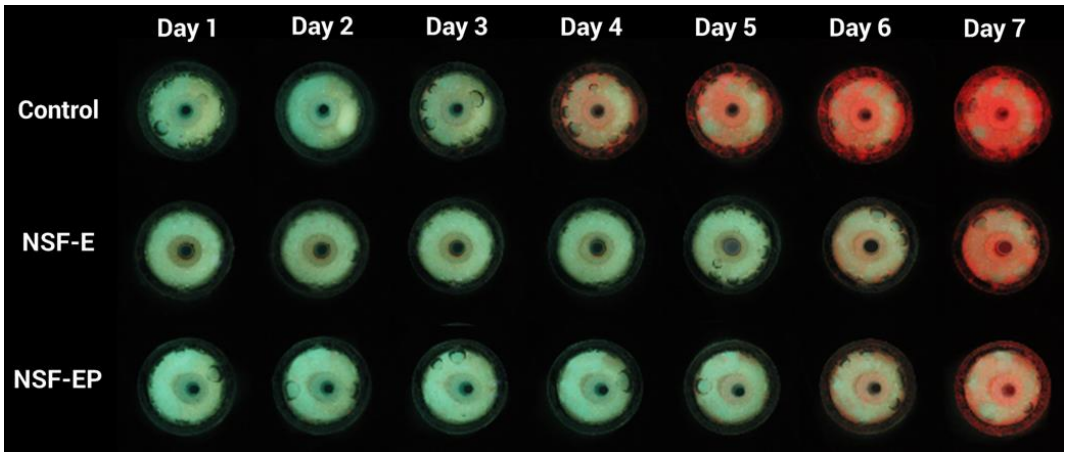

Figure 14. Fluorescence images of dental microcosm biofilms matured for 7-day under various treatments.

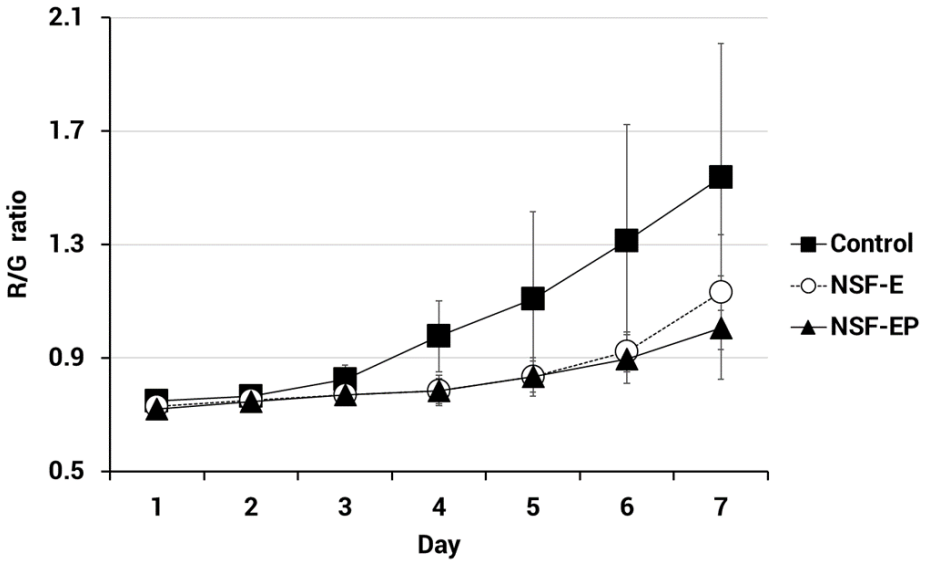

Figure 15. Changes in red/green ratio of dental microcosm biofilms grown in the different treatment groups according to maturation time.

3.3.2 Cell viability of dental microcosm biofilms

When the total bacteria and aciduric bacteria counts in 7-day mature biofilm were converted to Log_{10}CFU/ml, the NSF-E and NSF-EP groups showed reductions of 6.8% and 9.4%, respectively, in total bacteria compared to the control group ($P = 0.02$ and $P = 0.001$, respectively, Fig. 16, A). Additionally, aciduric bacteria decreased by 11.4% and 13.0%, respectively, compared to the control group ($P = 0.078$ and $P = 0.04$, respectively, Fig. 16, B)

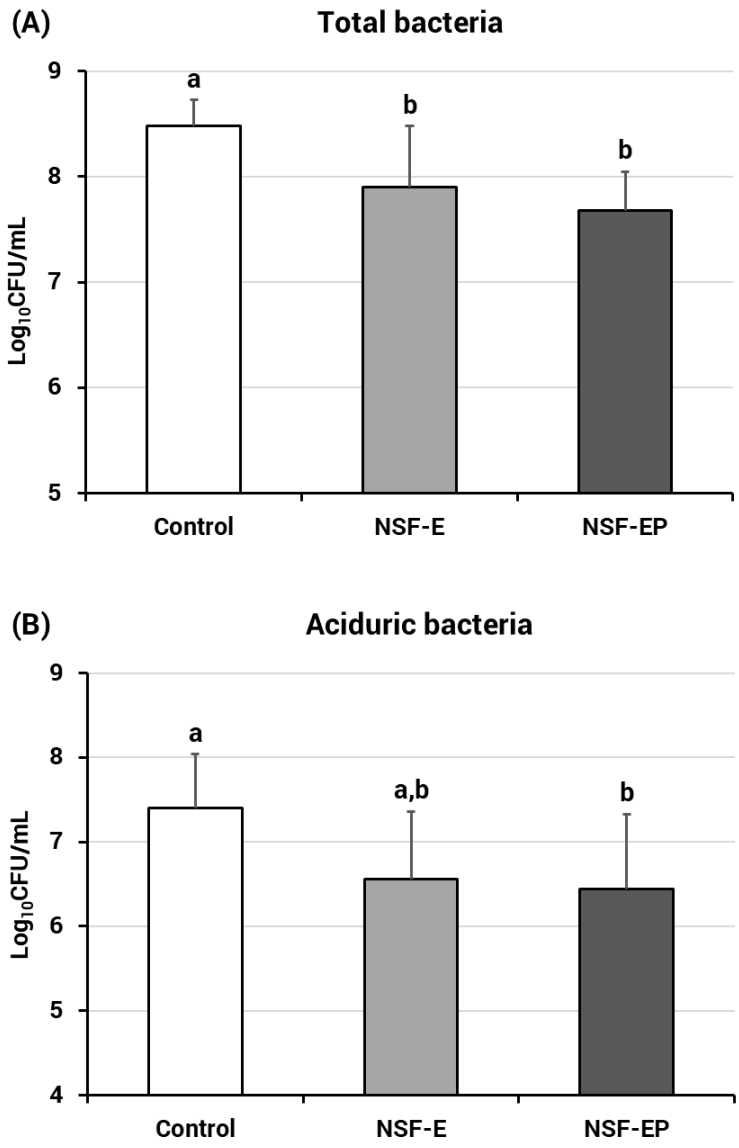

Figure 16. (A) Total viable and (B) Aciduric viable bacteria in 7-day mature dental microcosm biofilms grown in the different treatment groups. Different small letters (a, b) indicate significant differences between groups by ANOVA test with post hoc Tukey HSD test, $P < 0.05$; $n = 9$.

3.3.3 Thickness and live/dead cell ratio of dental microcosm biofilms

The thickness and live/dead cell ratio of the 7-day mature biofilm were observed using CLSM. The average thickness of the biofilm in the control group was 94.09 (standard deviation; 35.85) μm. Compared to the control group, the biofilm thickness reductions for NSF-E and NSF-EP were 34.9% and 36.1%, respectively, with both groups showing significantly reduced thickness (P = 0.043 and P = 0.036, respectively, Fig. 17, Table 4). For the live/dead cell ratio, NSF-E and NSF-EP exhibited increases of 14.9% and 3.0%, respectively, compared to the control group, which had a ratio of 0.67 (0.15). However, no significant differences were observed among all groups (Fig. 17, Table 4).

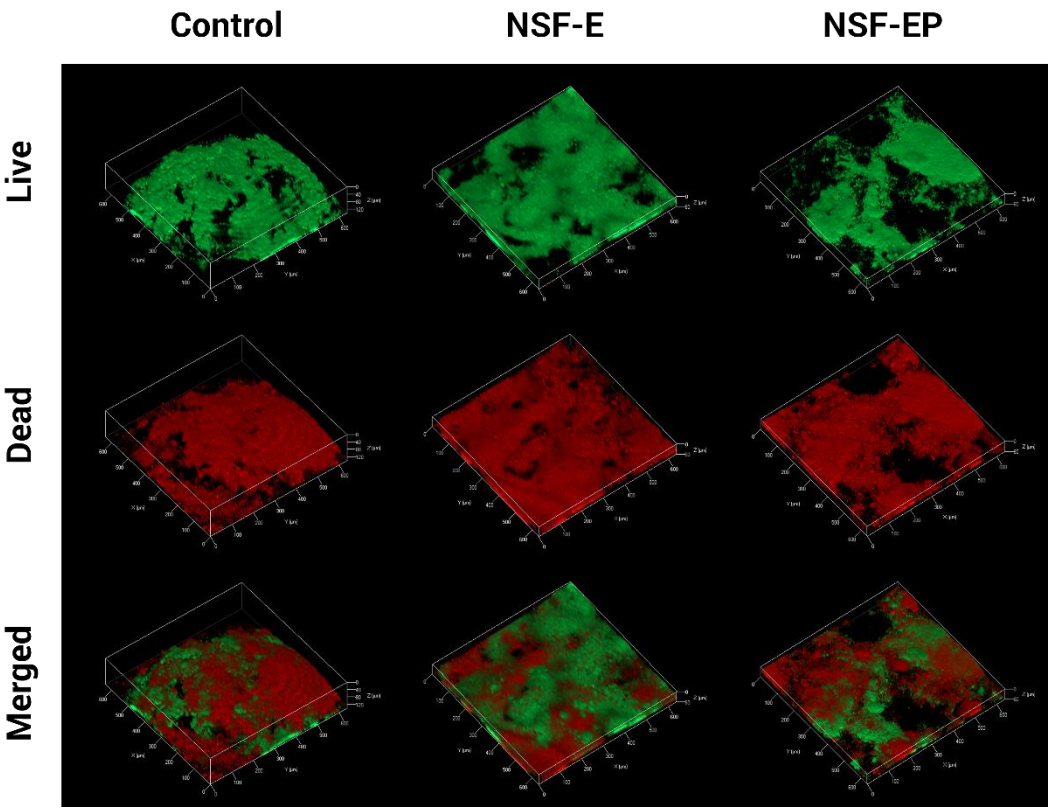

Figure 17. Confocal laser scanning microscopy images of live/dead cells on stained dental microcosm biofilms after 7 d in the different treatment groups.

Table 4. Quantitative analysis of thickness and live/dead cell ratio of each treated 7-day mature dental microcosm biofilms using COMSTAT (n = 10).

Groups	Thickness (μm)	Live/dead cell ratio
Control	94.09 (35.85)[a]	0.67 (0.15)[a]
NSF-E	61.25 (19.84)[b]	0.77 (0.29)[a]
NSF-EP	60.16 (28.66)[b]	0.69 (0.29)[a]

Data represent mean (standard deviation) values. NSF, nano silver fluoride; E, ethyl cellulose, EP; ethyl cellulose with polyethylene glycol 6000. Different small letters (a, b) within the same column indicate significant differences between groups by ANOVA test with post hoc Tukey HSD test (P < 0.05).

3.3.4 Changes of microbial profile in time

The alpha diversity of the biofilm was analyzed using the number of OTUs and the Shannon diversity index (Table 5). The results showed that as the biofilm matured, OTUs increased in all groups. The increase in OTUs was lower in NSF-E and NSF-EP compared to the control group, with NSF-EP showing the lowest OTUs during the biofilm maturation period. The Shannon diversity index results also indicated that diversity increased as the biofilm matured, with the control group showing the highest increase. There were no significant differences in the index among the groups (Table 5).

Comparing the changes in microbial composition among the groups using PCA plots, the saliva inoculum clustered separately from the biofilm, and NSF-E was closer to the control than NSF-EP (Fig. 18).

To analyze the microbial composition of biofilm treated with NSF-RE, biofilms matured for 3 and 7 days after saliva inoculation were sampled. The relative abundance (RA) of bacteria species with over 1% presence in the biofilm was presented, and other taxa were grouped as "other" (Fig. 19). *Streptococcus* and *Veillonella* were the most abundant genera in all microcosm biofilms.

Additionally, the RA of five bacteria known to be associated with dental caries (*Streptococcus mutans* and *Lactobacillus fermentum*) and those found in cariogenic dysbiotic biofilms (*Veillonella dispar*, *Veillonella atypica*, *Veillonella parvula*) were compared among the groups (Fig. 20). NSF-EP showed relatively lower RA for all five

bacteria in both 3-day and 7-day biofilms compared to the other groups. The highest RA in the 3-day mature biofilm treated with NSF-EP was observed for *Veillonella rogosae*, a potential biomarker of non-cariogenic oral microbiome, with RA of 2.1% and 2.3% in control and NSF-E treated biofilms, respectively.

Table 5. Number of OTUs and the Shannon diversity index of biofilms in different groups.

Groups	Number of OTUs		Shannon diversity index	
	Day 3	Day 7	Day 3	Day 7
Control	141 (16.97)[a]	283 (20.51)[a]	1.93 (0.03)[a]	2.30 (0.15)[a]
NSF-E	146 (83.44)[a]	195 (55.86)[a]	2.07 (0.13)[a]	2.11 (0.06)[a]
NSF-EP	93 (14.14)[a]	147 (46.67)[a]	2.10 (0.37)[a]	2.12 (0.06)[a]

Data represent mean (standard deviation) values. NSF, nano silver fluoride; E, ethyl cellulose, EP; ethyl cellulose with polyethylene glycol 6000. Different small letters within the same column indicate significant differences between groups by ANOVA test with post hoc Tukey HSD test ($P < 0.05$).

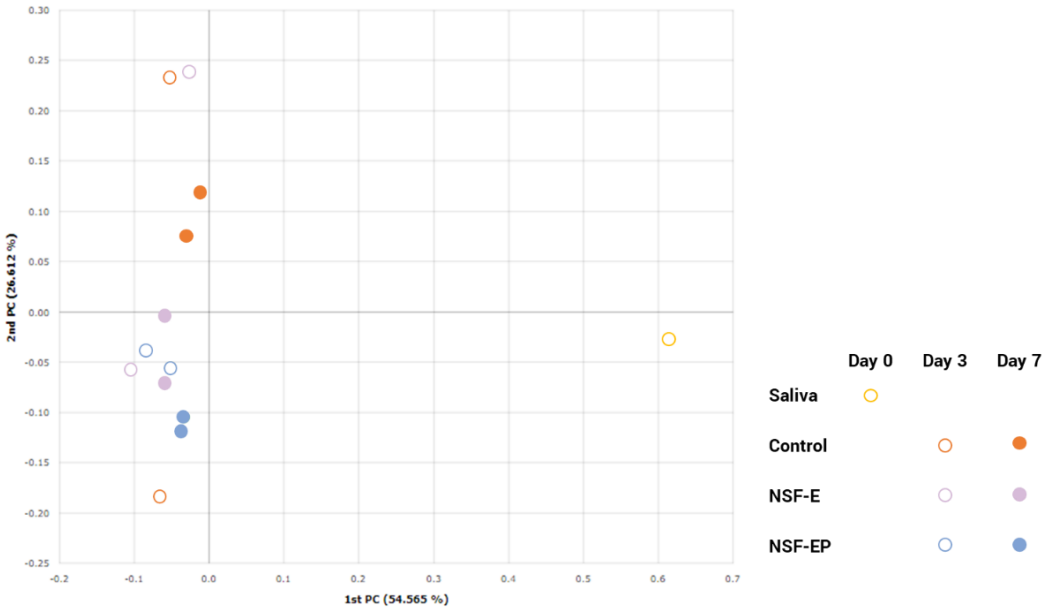

Figure 18. Principal component analysis (PCA) plots of saliva, day-3 (open symbols) and day-7 (filled symbols) dental microcosm biofilms in all groups.

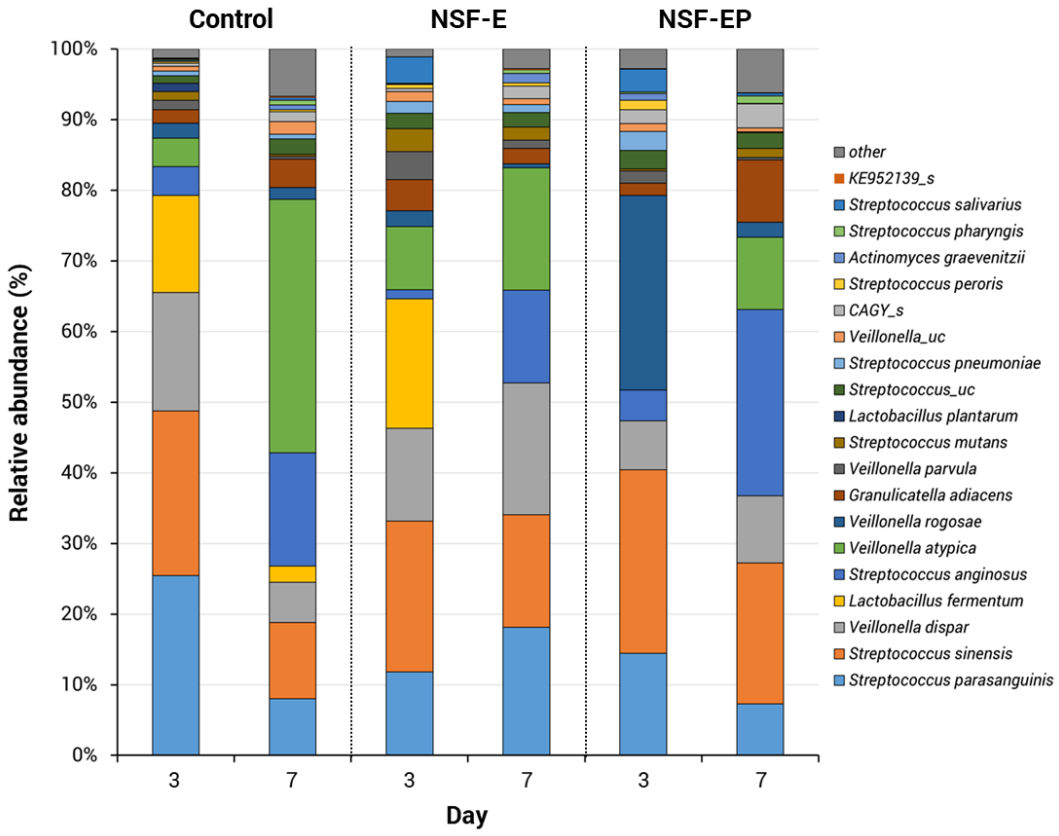

Figure 19. Relative abundance (average of replicates) of the top 20 most abundant bacterial species (remaining species are grouped as “other”) in day-3 and day-7 biofilms.

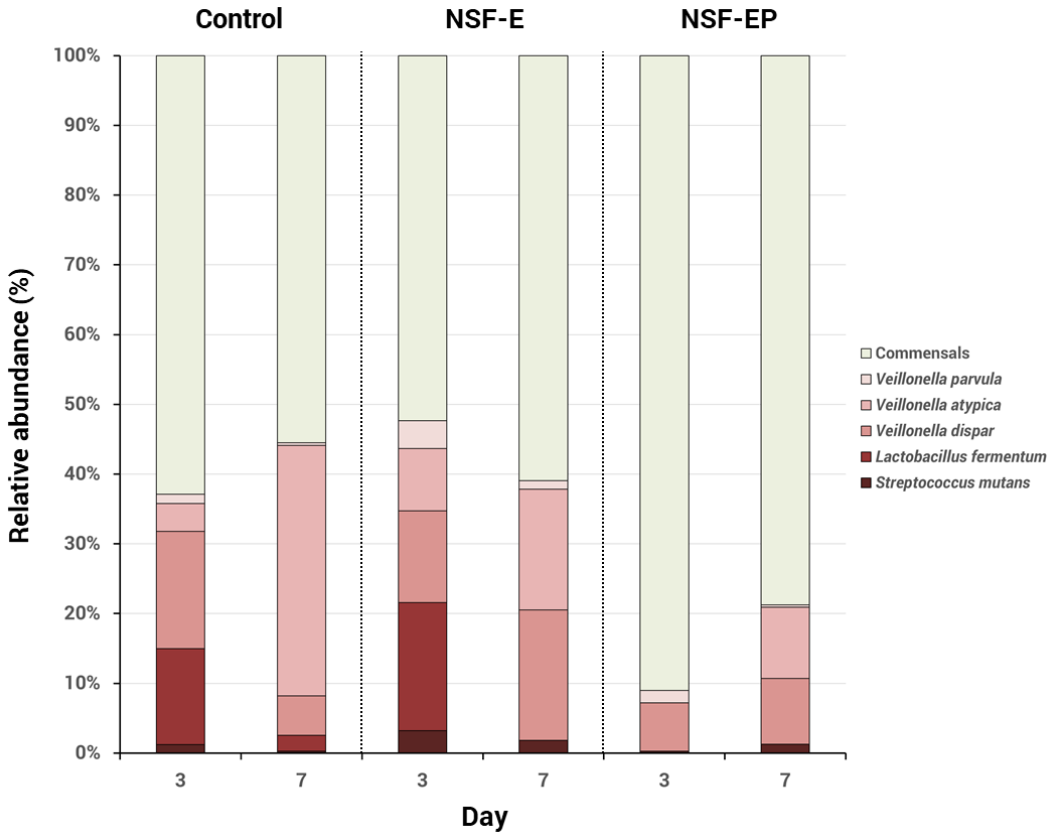

Figure 20. Relative abundance (average of replicates) of acidogenic and aciduric bacterial species in day-3 and day-7 biofilms.

3.3.5 Fluorescence loss of enamel specimen on QLF images

The ΔF (%) obtained from images taken with QLF-D reflects the percentage of mineral loss in enamel, enabling the quantification of WSLs. Evaluating the enamel under the 7-day mature biofilm with QLF revealed a loss of intrinsic fluorescence (Fig. 21). Compared to the control group, only the NSF-EP group showed a significant increase in ΔF (%) by 34.8% and ΔF_{max} by 38.7% ($P < 0.001$ and $P < 0.029$, respectively, Table 6). Evaluating the effective distance of AgNPs and fluoride released from the elastomerics using ΔΔF indicated that ΔΔF decreased as the distance from the elastomerics increased, but no significant differences were observed among all groups (Table 7).

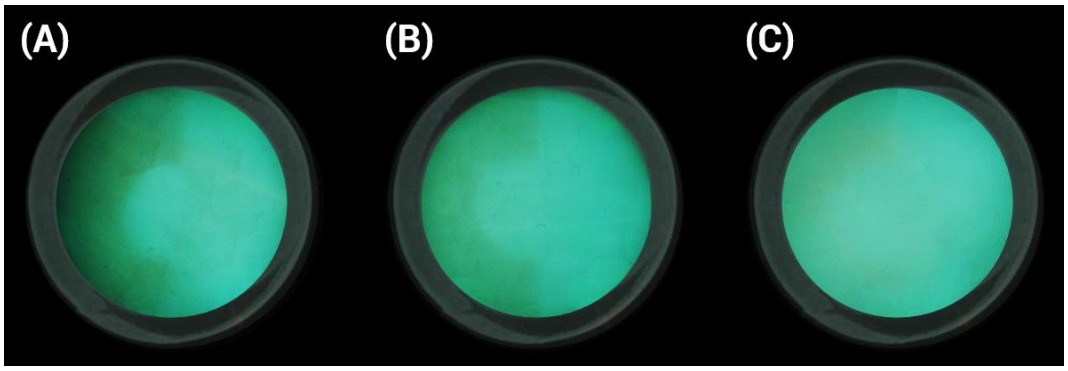

Figure 21. Fluorescence images of enamel discs under the 7-day mature dental microcosm biofilms according to treatment with (A) Control, (B) NSF-E, and (C) NSF-EP.

Table 6. ΔF (%) and ΔF_{max} (%) values in 7-day mature dental microcosm biofilms in the different treatment groups (n = 9).

Groups	**ΔF**	**ΔF_{max}**
Control	-14.92 (3.18)[a]	-26.38 (6.23)[a]
NSF-E	-13.14 (1.71)[a]	-22.53 (4.94)[a]
NSF-EP	-9.73 (1.76)[b]	-16.17 (3.09)[b]

Data represent mean (standard deviation) values. NSF, nano silver fluoride; E, ethyl cellulose, EP; ethyl cellulose with polyethylene glycol 6000. Different small letters (a, b) within the same column indicate significant differences between groups by ANOVA test with post hoc Tukey HSD test (P < 0.05).

Table 7. ΔΔF values based on distance from elastomerics attached to the specimen (n = 9).

Distance (mm)	ΔΔF	
	NSF-E	NSF-EP
0	2.23 (4.07)[a]	5.51 (5.62)[a]
1	1.43 (3.80)[a]	4.87 (4.81)[a]
2	1.33 (4.17)[a]	3.43 (3.86)[a]

Data represent mean (standard deviation) values. NSF, nano silver fluoride; E, ethyl cellulose, EP; ethyl cellulose with polyethylene glycol 6000. Different small letters within the same column indicate significant differences between groups by ANOVA test with post hoc Tukey HSD test (P < 0.05).

4. Discussion

In this study, we developed orthodontic elastomerics that continuously release AgNPs and fluoride to inhibit the formation of WSLs in orthodontic patients. The chemical and mechanical properties of the developed elastomerics were investigated. The clinical applicability of NSF-RE was evaluated through its anti-biofilm and demineralization-inhibiting effects on *S. mutans* and microcosm biofilms. The NSF-RE, coated with a solution combining EC and PEG, continuously released AgNPs and fluoride from the elastomeric surface for 7 days. The tensile strength of the coated elastomerics showed no statistically significant differences among the groups. Additionally, NSF-RE demonstrated antibacterial persistence effects against *S. mutans* and effectively inhibited the formation of *S. mutans* and microcosm biofilms. Particularly, the elastomeric coated with a solution composed of EC and PEG in a 2:1 ratio effectively inhibited enamel demineralization caused by multi-species biofilms. Therefore, applying orthodontic elastomerics coated with this solution could prevent WSLs caused by biofilm in orthodontic patients.

In the first study, we aimed to develop orthodontic elastomerics that continuously release AgNPs and fluoride to inhibit WSLs formation in orthodontic patients and to investigate their chemical and mechanical properties. The NSF-RE (NSF-E, NSF-EP1, and NSF-EP2) containing EC in the coating solution continuously released significantly higher amounts of AgNPs and fluoride for 7 days compared to the NSF group without EC. This is believed to be due to the formation of a matrix membrane formed by the EC film on the elastomeric

surface. EC, a hydrophobic polymer with excellent biocompatibility, can embed various antimicrobial substances such as AgNPs, tetracycline, and CHX (Joshi et al. 2016). Additionally, EC is known to induce the sustained release of embedded substances through aqueous pores and an osmotic pressure mechanism (Ozturk et al. 1990). Previous studies have shown that EC-coated wafers can continuously release approximately 30% of silver ions for 7 days (Bromberg, Buxton, and Friden 2001). Similarly, another study reported that local sustained release devices coated with EC continuously released about 40% of fluoride for 7 days (Shani, Friedman, and Steinberg 1998). Thus, EC can facilitate the sustained release of AgNPs and fluoride, as evidenced by the sustained release of CHX from elastomerics coated with a similar solution composition for 7 days in a previous study (Jeon et al. 2017).

In this study, among the three NSF-RE groups, the two groups with PEG added to the coating solution (NSF-EP1 and NSF-EP2) showed significantly higher cumulative release of AgNPs and fluoride. This is attributed to the plasticizer properties of PEG to EC. PEG is a nontoxic, water-soluble polymer with excellent biocompatibility and biodegradability. PEG is known to form pores when combined with other polymers and to promote interconnection between pore networks, thereby increasing the cumulative release of drugs (Palmer et al. 2011). According to a previous study, EC films containing PEG released more fluoride than films without PEG (Friedman 1980). In a previous study evaluating the release of metronidazole from EC-coated gelatin microspheres, the cumulative release of metronidazole increased with higher PEG concentrations (Phadke, Manjeshwar, and

Aminabhavi 2014). Furthermore, NSF-EP2, with a 2:1 ratio of EC to PEG in the coating solution, exhibited significantly higher cumulative release and faster release rates of AgNPs and fluoride compared to NSF-EP1, which had a 4:1 ratio. This is likely due to changes in the EC matrix structure depending on the PEG ratio. Previous studies evaluating the release of metoprolol tartrate from EC microspheres showed that the permeability of the EC matrix increased with higher PEG concentrations, resulting in faster release of metoprolol tartrate (Malipeddi, Awasthi, and Dua 2016). Similarly, a study on the release of metronidazole from EC films reported that higher PEG concentrations increased film permeability, leading to faster release of metronidazole (Golomb et al. 1984). Therefore, this study also confirmed that EC films with higher PEG concentrations resulted in greater cumulative release and faster release rates of AgNPs and fluoride.

To evaluate the mechanical properties of NSF-RE, we assessed the tensile strength of antimicrobial coatings elastomerics composed of NSF and EC. The results showed no significant differences in tensile strength among all groups regardless of coated or coating solution. This is attributed to the breaking stress of the EC matrix coating on the elastomeric surface being greater than the maximum tensile strength applied to the elastomeric (5.55N). Previous studies using the same casting solvent to produce EC film matrix without plasticizers showed a breaking stress of approximately 9.86 N/mm², while those with plasticizers ranged from 7.49 to 13.26 N/mm² (Hyppölä, Husson, and Sundholm 1996). Additionally, a previous study reported no differences in tensile strength between elastomerics coated with EC and those without, while evaluating the sustained release of

CHX from the elastomeric surface (Jeon et al. 2015). Therefore, orthodontic elastomerics coated with EC or EC-PEG mixtures do not affect the tensile strength required for attachment to orthodontic brackets.

In the second study, we evaluated the antibacterial persistence and inhibition of biofilm formation effects of NSF-RE against *S. mutans*, a well-known cariogenic bacteria. The antibacterial persistence effect of NSF-RE against *S. mutans* was evaluated by measuring the inhibition zone on day 7, and all NSF-coated elastomerics showed inhibition zones. This is attributed to the elastomeric surface being coated with AgNPs above the MIC. In a previous study evaluating the antibacterial efficacy of nano silver fluoride against *S. mutans* ATCC 25175, the MIC and MBC were 33.54 μg/mL and 50.32 μg/mL, respectively (dos Santos Junior et al. 2017). In this study, 92 μg/mL of AgNPs was applied to the elastomeric surface, resulting in the observed inhibition zones.

However, there were differences in the diameter of the inhibition zones among the groups, which is attributed to the differences in the cumulative release and release rate of AgNPs. A previous study evaluating the inhibition zones of *S. mutans* by elastomerics with sustained CHX release found that the diameter of the inhibition zones increased with the cumulative release of CHX (Jeon et al. 2017). Additionally, a previous study showed that EC films containing PEG exhibited a larger inhibition zone diameter over 27 days compared to films without PEG (Friedman et al. 1985). When applying antibacterial agents in the oral cavity using DDS, it is crucial to maintain an appropriate concentration that ensures both efficacy and safety. Therefore, NSF-EP2, which showed the highest

cumulative release of AgNPs for 7 days, is expected to be the most effective in preventing WSLs in orthodontic patients.

In this study, NSF-RE treated 64 h mature biofilms showed significantly lower CFUs, biofilm thickness, and live/dead cell ratio compared to the control group. This indicates that AgNPs released from NSF-RE effectively acted on *S. mutans* and maintained their activity throughout the biofilm formation period (64 h). AgNPs are known to attach to the cell wall and membrane of bacteria, inhibiting membrane permeability and inducing the loss of cellular components (Shrivastava et al. 2007). Additionally, AgNPs penetrate the bacteria, attaching to sulfur and phosphorus groups in DNA, leading to DNA damage (Hamed et al. 2017). The antibacterial activity of AgNPs is size-dependent, with nanoparticles of 1–10 nm diameter exhibiting strong antibacterial activity (Morones et al. 2005). The AgNPs produced in this study had an average diameter of 9.56 nm, resulting in strong antibacterial activity against *S. mutans*. A previous study evaluating the antibacterial persistence effect of orthodontic band cement releasing AgNPs (cumulative release of approximately 55 μg) showed antibacterial activity against *S. mutans* for up to 28 days (Moreira et al. 2015). Another study evaluating the biofilm inhibition effect of chitosan-stabilized AgNPs reported that AgNPs and chitosan inhibited the surface attachment of *S. mutans* and reduced biofilm thickness due to their strong antibacterial activity (Divakar et al. 2018). Additionally, a study evaluating the biofilm inhibition effect of nano silver fluoride containing 9.3 nm spherical AgNPs on *S. mutans* biofilm using CLSM found that it had a significant anti-biofilm effect, completely killing cell viability of biofilm (Freire et

al. 2015). In this study, the NSF group showed antibacterial persistence effects against *S. mutans* but did not inhibit the formation of *S. mutans* biofilm. NSF ceased releasing AgNPs within 48 h and showed 72%, 54%, and 44% lower cumulative release than NSF-E, NSF-EP1, and NSF-EP2, respectively. Therefore, its inhibitory effect on planktonic *S. mutans* before biofilm formation was low, and the additional release of AgNPs was insufficient during the biofilm formation and maturation process, leading to limited inhibition of *S. mutans* biofilm. This study confirmed that the combination of EC and PEG increased the cumulative release and duration of AgNPs release, especially when the PEG concentration in the EC film increased, promoting interconnection between pore networks and increasing the cumulative release of AgNPs. Thus, the sustained release of AgNPs from NSF-RE effectively showed antibacterial activity against *S. mutans* during the biofilm maturation period and inhibited the formation of single-species biofilms.

In the third study, we evaluated the anti-biofilm and demineralization-inhibiting effects of NSF-RE using an *in vitro* dental microcosm biofilm model. NSF-RE showed effective inhibition of microcosm biofilm formation through the sustained release of AgNPs and fluoride. Notably, NSF-EP, with a 2:1 ratio of EC to PEG in the coating solution, effectively inhibited demineralization compared to the control group. Therefore, using NSF-EP in orthodontic patients is expected to effectively prevent WSLs formation.

After 7 days of biofilm formation, the red fluorescence of NSF-RE was significantly lower than that of the control group, indicating inhibited biofilm maturation. QLF technology detects and quantifies biofilm maturation by showing red fluorescence of

endogenous metal-free fluorescent porphyrins. These porphyrins are formed during bacterial metabolism in the oral cavity when exposed to 405 nm blue visible light (Kim et al. 2014; Van der Veen et al. 2006). According to a previous study that evaluated the efficacy of antimicrobial agents using QLF technology, the R/G ratio, which represents red fluorescence values, decreased as the concentration of antimicrobial agents exposed to the biofilm increased (Lee et al. 2018). In this study, the decreased red fluorescence of NSF-RE compared to the control indicates that the sustained release of AgNPs from NSF-RE affected the composition and metabolic activity of secondary colonizers within the biofilm (Kim et al. 2014). Thus, the antimicrobial action of NSF-RE likely reduced the amount of red-fluorescing metabolites produced by bacterial metabolic interactions. This finding was supported by the changes in the microbial composition. During biofilm maturation, the composition of facultative anaerobes changes to obligate anaerobes (Coulthwaite et al. 2006; Han et al. 2019). In this study, the RA of *Veillonella* (a gram-negative obligate anaerobe) increased by 20.5% as the microcosm biofilms matured in the control group. Meanwhile, *Veillonella* decreased by 8.9% and 14.6% in the biofilms treated with NSF-E and NSF-EP, respectively. This indicates that NSF-RE effectively inhibited biofilm maturation.

Additionally, biofilms treated with NSF-RE showed a decrease in total and aciduric bacteria CFUs and biofilm thickness compared to the control. This suggests that the sustained release of AgNPs from NSF-RE effectively acted on microcosm biofilms throughout the maturation period (7 days). A previous study applying 0.4% stannous

fluoride gel to *in vivo* and *in vitro* polymicrobial biofilm models reported no significantly changes in plaque reduction and microbial composition (Reilly et al. 2014). Moreover, previous studies have shown that fluoride treatment did not exhibit significant anti-biofilm effects on microcosm biofilms (Hwang and Kim 2021; Souza et al. 2018). However, AgNPs could pass through the biofilm matrix and reach bacterial cells due to their small size, thereby exhibiting anti-biofilm effects (Di Giulio et al. 2013). Previous studies evaluating the antibacterial effect of AgNPs on subgingival plaque showed that AgNPs inhibited plaque maturation by approximately 17.4% (Espinosa-Cristóbal et al. 2019; Espinosa Cristobal 2021). The method of applying the antimicrobial agent also influenced the biofilm inhibition effect. A Study evaluating the regrowth of polymicrobial biofilms under mouthwash treatment found that CFUs of biofilm and lactic acid production recovered, and biofilm regrowth occurred within 2 days, regardless of the antimicrobial type and concentration (Han et al. 2019). Thus, our study confirmed that AgNPs continuously act on biofilms, which was also corroborated by the observed reduction in biofilm OTUs. It is known that antimicrobial treatment of biofilms reduces OTUs (Brookes et al. 2020; Mao et al. 2022). In our study, both NSF-E and NSF-EP showed lower OTUs on days 3 and 7 and a reduced increase rate in OTUs (day 3 to day 7) compared to the control. This indicates that NSF-RE, which releases AgNPs has a continuous antibacterial effect on polymicrobial biofilms, effectively inhibiting biofilm formation.

NSF-E and NSF-EP significantly inhibited the formation of *S. mutans* biofilm, but only NSF-EP showed a significantly antibacterial effect on aciduric bacteria in dental

microcosm biofilms. This is likely due to the higher resistance of polymicrobial biofilms to antimicrobial agents compared to single-species biofilms. Polymicrobial biofilms can enhance their structure and increase antimicrobial resistance through quorum signaling and metabolic cooperation (Elias and Banin 2012). A study comparing the antimicrobial resistance of single and dual species biofilms of *S. mutans* and *V. parvula* showed significantly higher resistance in dual species biofilms compared to single-species biofilms (Kara, Luppens, and ten Cate 2006). Therefore, the biofilm inhibition effect of NSF-RE was lower in dental microcosm biofilms formed with saliva as the inoculum, and among NSF-RE groups, NSF-EP, which had 44.2% higher cumulative release of AgNPs, exhibited a more significantly anti-biofilm effect.

A notable finding of this study is that the microbial composition of biofilms treated with NSF-RE did not shift towards pathogenicity. Recent studies evaluating the effects of antimicrobial agents on the microbial composition of *in vitro* dental biofilms have reported an increase in the abundance of pathogenic microorganisms due to antimicrobial use (Chatzigiannidou et al. 2020; Zayed et al. 2022). Additionally, the change in microbial composition of biofilms can vary depending on the type of antimicrobial agent. A previous study which treated *in vitro* dental biofilms with CHX and CPC for 7 days under mouthwash treatment, found that the abundance of taxa related to dental caries increased in CHX-treated biofilms, while the abundance of taxa related to gingivitis increased in CPC-treated biofilms (Mao et al. 2022). Furthermore, recent studies have indicated that the use of CHX, known as the gold standard antimicrobial, can shift the normal flora to

pathogenic microbiota (Brookes et al. 2020). In contrast, in this study, the biofilms matured for 3 days treated with NSF-EP had a 28.2% lower total RA of bacteria associated with dental caries (*S. mutans*, *L. fermentum*, *V. dispar*, *V. atypica*, *V. parvula*) compared to the control, and a 23.2% lower RA on day 7. Additionally, the Shannon diversity of NSF-RE showed no significantly difference from the control, indicating that NSF-RE does not reduce biofilm diversity. According to ecological theory, communities with high richness of bacterial species are healthier and more resilient to disturbances than those with low richness of bacterial species (Levine and D'Antonio 1999). Thus, reduced biofilm diversity can increase the risk of oral diseases (Chatzigiannidou et al. 2020). Therefore, from an anti-biofilm perspective, NSF-RE effectively inhibits biofilm formation without shifting the microbial composition towards pathogenicity.

Using QLF to evaluate the mineral loss formed under the biofilm matured for 7 days, it was found that the ΔF and ΔF_{max} of the specimens treated with NSF-EP were significantly higher than that of the negative control group. This confirms the demineralization-inhibiting effect of NSF-EP. The fluorescence loss (ΔF, ΔF_{max}) detected by QLF is an indicator for assessing the degree of demineralization of the teeth and enables the quantification of white spot lesions (Choi et al. 2022; Van der Veen and de Jong 2000). The demineralization inhibition of the specimens treated with NSF-EP is attributed to the fluoride released from NSF-RE acting on the enamel to form CaF_2 before biofilm formation. A previous study evaluating the enamel remineralization efficacy of fluoride in the presence of biofilm indicated that fluoride efficacy was significantly reduced in the presence of

biofilm (Kang and Kim 2021). Another study evaluating the demineralization inhibition effect of CaF_2 formed on enamel without biofilm reported a high correlation (r = -0.75) between fluoride release and enamel demineralization inhibition (Tenuta et al. 2008). In this study, the demineralization-inhibiting effect is considered to result from the fluoride released from NSF-RE acting on the specimen surface before biofilm formation. Additionally, a previous study evaluating the cumulative fluoride release of 5% NaF varnish (Duraphat®) applied to specimens of the same size (8 mm x 8 mm) as in this study found that approximately 39.44 ppm of fluoride was released for 7 days, with about 69.5% released within 24 h (Piesiak-Panczyszyn et al. 2023). A previous study reported that after maturing microcosm biofilms on the enamel surface treated with 5.42% NaF varnish for 14 days, the lesion depth was approximately 44.3% shallower (Souza et al. 2018). In this study, the specimens combined with NSF-EP cumulatively released about 27.6 ppm of fluoride for 7 days, with about 86.0% released within 24 h. Although the amount was relatively lower than that of the fluoride varnish, it effectively inhibited demineralization (ΔF increased by approximately 34.8%; lesion depth decreased by approximately 23.3%).

The ΔF and ΔF_{max} of specimens treated with NSF-E were lower than that of NSF-EP, which is attributed to the cumulative fluoride release for 7 days being 21.3% less than NSF-EP, with about 88.1% of fluoride being rapidly released within 24 h. Additionally, the RA of the cariogenic bacteria on day 3 of biofilm formation was higher in NSF-E, which is believed to have influenced the ΔF and ΔF_{max}. The greater anti-biofilm effect of NSF-EP is also thought to have contributed to the ΔF and ΔF_{max}. AgNPs enhance antibacterial activity

in acidic environments and exhibit strong antibacterial effects on polymicrobial biofilms. A previous study evaluating the antibacterial effect of AgNPs on *Lactobacilli* reported that the acidic growth environment of *Lactobacilli* promotes AgNPs dissolution, excessive hydroxyl radical production, and increased intracellular ROS, resulting in high antibacterial activity (Tian et al. 2018). Additionally, a previous RCT study evaluating the biofilm microbial composition of dental caries lesions in primary dentin after 1 month of NSF application found that *S. mutans* decreased by 21.3% and *Lactobacilli* by 13.9% (Ammar et al. 2022). Therefore, the higher demineralization-inhibiting effect observed in NSF-EP is attributed to the 52.7% greater AgNPs release within 12 h and the 44.2% greater cumulative release for 7 days. Thus, AgNPs and fluoride released from NSF-EP act on the biofilm, exhibiting anti-biofilm effects and effectively inhibiting enamel demineralization.

For the clinical use of NSF-RE, safety is a crucial factor. This study found that NSF-RE released approximately 64 ppm of AgNPs and 9 ppm of fluoride for 7 days. Previous research evaluating the hemolytic activity of NSF on human erythrocytes reported that a 100 μg/mL concentration of nano silver fluoride colloid did not exhibit toxicity to any type of erythrocyte (Targino et al. 2014). Another study evaluating the biocompatibility of silk fibroin membranes coated with nano silver fluoride reported no cytotoxicity to mouse fibroblast cell lines (L929 cell line) (Pandey et al. 2021). However, for the clinical application of NSF-RE, *in vivo* studies are necessary. Additionally, a limitation of this study is that the anti-biofilm and demineralization-inhibiting effects of NSF-RE were evaluated for only 7 days. Orthodontic elastomerics used as ligature materials typically have a

replacement cycle of about 30 days. A previous clinical study evaluating the sustained antibacterial effect of orthodontic ligature elastomerics releasing CHX for 7 days reported that, 28 days after ligation, *S. mutans* in saliva decreased by approximately 80%, and *S. mutans* on the elastomeric surface also significantly decreased by 50% compared to the control group (Mehrabi, Feizbakhsh, and Tahmorespour 2021). Thus, it is believed that antimicrobial agents continue to act on the oral cavity and the elastomeric surface for about 30 days after the release period. However, additional evaluations of the demineralization-inhibiting effect and sustainability of AgNPs and fluoride released from NSF-RE in the actual oral environment are needed. Moreover, while this study focused on elastomerics as ligature materials for brackets, the specimens used were in a form where elastomerics were attached to the surface. Although the study results of calculating the ΔΔF of the specimens based on the distance from the elastomerics confirmed that the active substances acted throughout the specimen, the study could not directly confirm the effect of the active substances on the distance between the bracket and the enamel surface.

Although this study evaluated the anti-biofilm and demineralization-inhibiting effects of NSF-coated orthodontic ligature elastomerics, it is believed that the coating method can also be applied to elastics used in class III orthodontic treatment or separator elastics used in interdental separation. This could effectively prevent oral diseases occurring during orthodontic treatment or biofilm-related diseases induced by elastomerics.

5. Conclusion

The NSF-EP (EC:PEG/2:1) developed through this study released the highest amounts of AgNPs and fluoride for 7 days compared to elastomerics coated with other solution compositions. Furthermore, there was no significant difference in tensile strength compared to regular elastomerics, indicating its applicability to orthodontic brackets.

NSF-RE effectively inhibited the formation of *S. mutans* and dental microcosm biofilms, with NSF-EP, which had the highest fluoride release, showing significant inhibition of enamel demineralization. Based on these results, using NSF-RE could enable orthodontic patients to manage oral hygiene easily and effectively, thereby preventing the formation of WSLs caused by biofilm.

References

Aas JA, Paster BJ, Stokes LN, Olsen I, Dewhirst FE: Defining the normal bacterial flora of the oral cavity. *Journal of clinical microbiology* 43(11):5721-5732, 2005.

Ahmed F, Prashanth ST, Sindhu K, Nayak A, Chaturvedi S: Antimicrobial efficacy of nanosilver and chitosan against Streptococcus mutans, as an ingredient of toothpaste formulation: An in vitro study. *J Indian Soc Pedod Prev Dent* 37(1):46-54, 2019.

Al-Tannir MA, Goodman HS: A review of chlorhexidine and its use in special populations. *Special Care in Dentistry* 14(3):116-122, 1994.

Ammar N, El-Tekeya MM, Essa S, Essawy MM, Talaat DM: Antibacterial effect and impact on caries activity of nanosilver fluoride and silver diamine fluoride in dentin caries of primary teeth: a randomized controlled clinical trial. *BMC Oral Health* 22(1):657, 2022.

Arnaud TM, de Barros Neto B, Diniz FB: Chitosan effect on dental enamel de-remineralization: an in vitro evaluation. *J Dent* 38(11):848-852, 2010.

Bolger AM, Lohse M, Usadel B: Trimmomatic: a flexible trimmer for Illumina sequence data. *Bioinformatics* 30(15):2114-2120, 2014.

Bowen WH, Koo H: Biology of Streptococcus mutans-derived glucosyltransferases: role in extracellular matrix formation of cariogenic biofilms. *Caries Res* 45(1):69-86, 2011.

Bromberg LE, Buxton DK, Friden PM: Novel periodontal drug delivery system for treatment of periodontitis. *Journal of controlled release* 71(3):251-259, 2001.

Brookes ZL, Bescos R, Belfield LA, Ali K, Roberts A: Current uses of chlorhexidine for management of oral disease: a narrative review. *Journal of dentistry* 103:103497, 2020.

Chapman JA, Roberts WE, Eckert GJ, Kula KS, Gonzalez-Cabezas C: Risk factors for incidence and severity of white spot lesions during treatment with fixed orthodontic appliances. *Am*

J Orthod Dentofacial Orthop 138(2):188-194, 2010.

Chatzigiannidou I, Teughels W, Van de Wiele T, Boon N: Oral biofilms exposure to chlorhexidine results in altered microbial composition and metabolic profile. *npj Biofilms and Microbiomes* 6(1):13, 2020.

Choi JH, Jung EH, Lee ES, Jung HI, Kim BI: Anti-biofilm activity of chlorhexidine-releasing elastomerics against dental microcosm biofilms. *J Dent* 122:104153, 2022.

Coulthwaite L, Pretty IA, Smith PW, Higham SM, Verran J: The microbiological origin of fluorescence observed in plaque on dentures during QLF analysis. *Caries research* 40(2):112-116, 2006.

Di Giulio M, Di Bartolomeo S, Di Campli E, Sancilio S, Marsich E, Travan A, et al.: The effect of a silver nanoparticle polysaccharide system on streptococcal and saliva-derived biofilms. *International journal of molecular sciences* 14(7):13615-13625, 2013.

Divakar DD, Jastaniyah NT, Altamimi HG, Alnakhli YO, Muzaheed, Alkheraif AA, et al.: Enhanced antimicrobial activity of naturally derived bioactive molecule chitosan conjugated silver nanoparticle against dental implant pathogens. *International Journal of Biological Macromolecules* 108:790-797, 2018.

dos Santos Junior VE, Targino AGR, Flores MAP, Rodríguez-Díaz JM, Teixeira JA, Heimer MV, et al.: Antimicrobial activity of silver nanoparticle colloids of different sizes and shapes against Streptococcus mutans. *Research on Chemical Intermediates* 43(10):5889-5899, 2017.

Edgar RC, Haas BJ, Clemente JC, Quince C, Knight R: UCHIME improves sensitivity and speed of chimera detection. *Bioinformatics* 27(16):2194-2200, 2011.

Elias S, Banin E: Multi-species biofilms: living with friendly neighbors. *FEMS microbiology reviews* 36(5):990-1004, 2012.

Espinosa-Cristóbal LF, Holguín-Meráz C, Zaragoza-Contreras EA, Martínez-Martínez RE, Donohue-Cornejo A, Loyola-Rodríguez JP, et al.: Antimicrobial and substantivity properties of silver nanoparticles against oral microbiomes clinically isolated from young and young-adult patients. *Journal of Nanomaterials* 2019:1-14, 2019.

Espinosa Cristobal LF: Antimicrobial Activity of Silver Nanoparticles against Clinical Biofilms from Patients with and without Dental Caries. *Instituto de Ciencias Biomédicas*, 2021.

Freire PL, Stamford TC, Albuquerque AJ, Sampaio FC, Cavalcante HM, Macedo RO, et al.: Action of silver nanoparticles towards biological systems: cytotoxicity evaluation using hen's egg test and inhibition of Streptococcus mutans biofilm formation. *Int J Antimicrob Agents* 45(2):183-187, 2015.

Friedman M: Fluoride Prolonged Release Preparations for Topical Use. *Journal of Dental Research* 59(8):1392-1397, 1980.

Friedman M, Harari D, Raz H, Golomb G, Brayer L: Plaque Inhibition by Sustained-Release of Chlorhexidine from Removable Appliances. *Journal of Dental Research* 64(11):1319-1321, 1985.

Golomb G, Friedman M, Soskolne A, Stabholz A, Sela MN: Sustained-Release Device Containing Metronidazole for Periodontal Use. *Journal of Dental Research* 63(9):1149-1153, 1984.

Guggenheim B, Guggenheim M, Gmur R, Giertsen E, Thurnheer T: Application of the Zurich biofilm model to problems of cariology. *Caries Res* 38(3):212-222, 2004.

Gultom FP, Khoirunnisa N, Sahlan M, Soekanto SA: Evaluation of the potential of Nano Silver Fluoride against Streptococcus mutans and Enterobacter faecalis in various stages of biofilm maturation. In: *AIP Conference Proceedings*. AIP Publishing. 2019.

Haas AN, Pannuti CM, Andrade AKPd, Escobar EC, Almeida ERd, Costa FO, et al.: Mouthwashes for the control of supragingival biofilm and gingivitis in orthodontic patients: evidence-

based recommendations for clinicians. *Brazilian oral research* 28:1-8, 2014.

Hall CW, Mah T-F: Molecular mechanisms of biofilm-based antibiotic resistance and tolerance in pathogenic bacteria. *FEMS microbiology reviews* 41(3):276-301, 2017.

Hamed S, Emara M, Shawky RM, El-domany RA, Youssef T: Silver nanoparticles: Antimicrobial activity, cytotoxicity, and synergism with N-acetyl cysteine. *Journal of Basic Microbiology* 57(8):659-668, 2017.

Han Q, Jiang Y, Brandt BW, Yang J, Chen Y, Buijs MJ, et al.: Regrowth of microcosm biofilms on titanium surfaces after various antimicrobial treatments. *Frontiers in microbiology* 10:2693, 2019.

Heymann GC, Grauer D: A contemporary review of white spot lesions in orthodontics. *J Esthet Restor Dent* 25(2):85-95, 2013.

Hwang H-Y, Kim H-E: Influence of a novel pH-cycling model using dental microcosm biofilm on the remineralizing efficacy of fluoride in early carious lesions. *Clinical Oral Investigations* 25:337-344, 2021.

Hyppölä R, Husson I, Sundholm F: Evaluation of physical properties of plasticized ethyl cellulose films cast from ethanol solution Part I. *International journal of pharmaceutics* 133(1-2):161-170, 1996.

Jeon HS, Choi CH, Kang SM, Kwon HK, Kim BI: Chlorhexidine-releasing orthodontic elastomerics. *Dent Mater J* 34(3):321-326, 2015.

Jeon HS, Jung EH, Kang SM, Lee ES, Lee JW, Kim BI: Improving the efficacy of chlorhexidine-releasing elastomerics using a layer-by-layer coating technique. *Dent Mater J* 36(4):476-481, 2017.

Joshi D, Garg T, Goyal AK, Rath G: Advanced drug delivery approaches against periodontitis. *Drug Deliv* 23(2):363-377, 2016.

Kang M-K, Kim H-E: Remineralizing efficacy of fluoride in the presence of oral microcosm biofilms. *Journal of Dentistry* 115:103848, 2021.

Kang S-M, Jeong S-H, Kim H-E, Kim B-I: Photodiagnosis of White Spot Lesions after Orthodontic Treatment with a Quantitative Light-induced Fluorescence-Digital System: A Pilot Study. *Oral Health & Preventive Dentistry* 15(5), 2017.

Kara D, Luppens SB, ten Cate JM: Differences between single-and dual-species biofilms of Streptococcus mutans and Veillonella parvula in growth, acidogenicity and susceptibility to chlorhexidine. *European journal of oral sciences* 114(1):58-63, 2006.

Kim Y-S, Lee E-S, Kwon H-K, Kim B-I: Monitoring the maturation process of a dental microcosm biofilm using the Quantitative Light-induced Fluorescence-Digital (QLF-D). *Journal of dentistry* 42(6):691-696, 2014.

Lee E-S, De Jong EDJ, Jung H-I, Kim B-I: Red fluorescence of dental biofilm as an indicator for assessing the efficacy of antimicrobials. *Journal of biomedical optics* 23(1):015003, 2018.

Levine JM, D'Antonio CM: Elton revisited: a review of evidence linking diversity and invasibility. *Oikos*:15-26, 1999.

Liang J, Peng X, Zhou X, Zou J, Cheng L: Emerging Applications of Drug Delivery Systems in Oral Infectious Diseases Prevention and Treatment. *Molecules* 25(3), 2020.

Lucchese A, Bondemark L, Marcolina M, Manuelli M: Changes in oral microbiota due to orthodontic appliances: a systematic review. *Journal of oral microbiology* 10(1):1476645, 2018.

Malipeddi VR, Awasthi R, Dua K: Formulation and evaluation of controlled release ethylcellulose and polyethylene glycol microspheres containing metoprolol tartrate. *Interv Med Appl Sci* 8(2):60-67, 2016.

Mao X, Hiergeist A, Auer DL, Scholz KJ, Muehler D, Hiller K-A, et al.: Ecological effects of daily

antiseptic treatment on microbial composition of saliva-grown microcosm biofilms and selection of resistant phenotypes. *Frontiers in Microbiology* 13:934525, 2022.

Marsh P: Controlling the oral biofilm with antimicrobials. *Journal of dentistry* 38:S11-S15, 2010.

Marsh PD, Bradshaw DJ: Dental Plaque as a Biofilm. *Journal of Industrial Microbiology* 15(3):169-175, 1995.

Mehrabi S, Feizbakhsh M, Tahmorespour A: Effect of chlorhexidine-releasing elastomeric ligatures on Streptococcus mutans count in orthodontic patients: A clinical trial. *European Journal of Molecular and Clinical Medicine* 8(1):1921-1930, 2021.

Miura KK, Ito IY, Enoki C, Elias AM, Matsumoto MA: Anticariogenic effect of fluoride-releasing elastomers in orthodontic patients. *Braz Oral Res* 21(3):228-233, 2007.

Moreira DM, Oei J, Rawls HR, Wagner J, Chu L, Li Y, et al.: A novel antimicrobial orthodontic band cement with in situ-generated silver nanoparticles. *Angle Orthod* 85(2):175-183, 2015.

Morones JR, Elechiguerra JL, Camacho A, Holt K, Kouri JB, Ramirez JT, et al.: The bactericidal effect of silver nanoparticles. *Nanotechnology* 16(10):2346-2353, 2005.

Mummolo S, Tieri M, Nota A, Caruso S, Darvizeh A, Albani F, et al.: Salivary concentrations of Streptococcus mutans and Lactobacilli during an orthodontic treatment. An observational study comparing fixed and removable orthodontic appliances. *Clin Exp Dent Res* 6(2):181-187, 2020.

Myers EW, Miller W: Optimal alignments in linear space. *Bioinformatics* 4(1):11-17, 1988.

Ozturk AG, Ozturk SS, Palsson BO, Wheatley TA, Dressman JB: Mechanism of Release from Pellets Coated with an Ethylcellulose-Based Film. *Journal of Controlled Release* 14(3):203-213, 1990.

Palmer D, Levina M, Nokhodchi A, Douroumis D, Farrell T, Rajabi-Siahboomi A: The influence of sodium carboxymethylcellulose on drug release from polyethylene oxide extended release

matrices. *AAPS PharmSciTech* 12(3):862-871, 2011.

Pandey A, Yang TS, Yang TI, Belem WF, Teng NC, Chen IW, et al.: An Insight into Nano Silver Fluoride-Coated Silk Fibroin Bioinspired Membrane Properties for Guided Tissue Regeneration. *Polymers (Basel)* 13(16), 2021.

Phadke KV, Manjeshwar LS, Aminabhavi TM: Microspheres of Gelatin and Poly(ethylene glycol) Coated with Ethyl Cellulose for Controlled Release of Metronidazole. *Industrial & Engineering Chemistry Research* 53(16):6575-6584, 2014.

Piesiak-Panczyszyn D, Watras A, Wiglusz RJ, Dobrzynski M: In Vitro Comparison of the Fluoride Ion Release from the First-and Second-Generation Fluoride Varnishes. *Applied Sciences* 13(12):7327, 2023.

Pithon MM, Sant'Anna LIDA, Baião FCS, dos Santos RL, da Silva Coqueiro R, Maia LC: Assessment of the effectiveness of mouthwashes in reducing cariogenic biofilm in orthodontic patients: a systematic review. *Journal of dentistry* 43(3):297-308, 2015.

Pushpalatha C, Bharkhavy KV, Shakir A, Augustine D, Sowmya SV, Bahammam HA, et al.: The Anticariogenic Efficacy of Nano Silver Fluoride. *Front Bioeng Biotechnol* 10:931327, 2022.

Reilly C, Rasmussen K, Selberg T, Stevens J, Jones RS: Biofilm community diversity after exposure to 0· 4% stannous fluoride gels. *Journal of applied microbiology* 117(6):1798-1809, 2014.

Ren Y, Jongsma MA, Mei L, van der Mei HC, Busscher HJ: Orthodontic treatment with fixed appliances and biofilm formation--a potential public health threat? *Clin Oral Investig* 18(7):1711-1718, 2014.

Rognes T, Flouri T, Nichols B, Quince C, Mahé F: VSEARCH: a versatile open source tool for metagenomics. *PeerJ* 4:e2584, 2016.

Rosenbloom RG, Tinanoff N: Salivary Streptococcus-Mutans Levels in Patients before, during, and

after Orthodontic Treatment. *American Journal of Orthodontics and Dentofacial Orthopedics* 100(1):35-37, 1991.

Santos VE, Jr., Vasconcelos Filho A, Targino AG, Flores MA, Galembeck A, Caldas AF, Jr., et al.: A new "silver-bullet" to treat caries in children--nano silver fluoride: a randomised clinical trial. *J Dent* 42(8):945-951, 2014.

Shani S, Friedman M, Steinberg D: In vitro assessment of the antimicrobial activity of a local sustained release device containing amine fluoride for the treatment of oral infectious diseases. *Diagnostic microbiology and infectious disease* 30(2):93-97, 1998.

Shrivastava S, Bera T, Roy A, Singh G, Ramachandrarao P, Dash D: Characterization of enhanced antibacterial effects of novel silver nanoparticles. *Nanotechnology* 18(22):225103-225500, 2007.

Souza BMd, Fernandes Neto C, Salomão PMA, Vasconcelos LRSMd, Andrade FBd, Magalhães AC: Analysis of the antimicrobial and anti-caries effects of TiF 4 varnish under microcosm biofilm formed on enamel. *Journal of Applied Oral Science* 26, 2018.

Storie DJ, Regennitter F, Vonfraunhofer JA: Characteristics of a Fluoride-Releasing Elastomeric Chain. *Angle Orthodontist* 64(3):199-210, 1994.

Sudjalim TR, Woods MG, Manton DJ: Prevention of white spot lesions in orthodontic practice: a contemporary review. *Aust Dent J* 51(4):284-289; quiz 347, 2006.

Targino AG, Flores MA, dos Santos Junior VE, de Godoy Bene Bezerra F, de Luna Freire H, Galembeck A, et al.: An innovative approach to treating dental decay in children. A new anti-caries agent. *J Mater Sci Mater Med* 25(8):2041-2047, 2014.

ten Cate JM: Current concepts on the theories of the mechanism of action of fluoride. *Acta Odontol Scand* 57(6):325-329, 1999.

Tenuta L, Cerezetti R, Del Bel Cury A, Tabchoury C, Cury J: Fluoride release from CaF2 and enamel

demineralization. *Journal of dental research* 87(11):1032-1036, 2008.

Tian X, Jiang X, Welch C, Croley TR, Wong T-Y, Chen C, et al.: Bactericidal effects of silver nanoparticles on lactobacilli and the underlying mechanism. *ACS applied materials & interfaces* 10(10):8443-8450, 2018.

Topaloglu-Ak A, Ertugrul F, Eden E, Ates M, Bulut H: Effect of Orthodontic Appliances on Oral Microbiota-6 Month Follow-up. *Journal of Clinical Pediatric Dentistry* 35(4):433-436, 2011.

Van der Veen M, de Jong EdJ: Application of quantitative light-induced fluorescence for assessing early caries lesions. *Monogr Oral Sci* 17:144-162, 2000.

Van der Veen M, Thomas R, Huysmans M, De Soet J: Red autofluorescence of dental plaque bacteria. *Caries research* 40(6):542-545, 2006.

Wheeler TJ, Eddy SR: nhmmer: DNA homology search with profile HMMs. *Bioinformatics* 29(19):2487-2489, 2013.

Wong L, Sissions C: A comparison of human dental plaque microcosm biofilms grown in an undefined medium and a chemically defined artificial saliva. *Archives of oral biology* 46(6):477-486, 2001.

Yoon S-H, Ha S-M, Kwon S, Lim J, Kim Y, Seo H, et al.: Introducing EzBioCloud: a taxonomically united database of 16S rRNA gene sequences and whole-genome assemblies. *International journal of systematic and evolutionary microbiology* 67(5):1613-1617, 2017.

Zaura-Arite E, Van Marle J, Ten Cate J: Confocal microscopy study of undisturbed and chlorhexidine-treated dental biofilm. *Journal of dental research* 80(5):1436-1440, 2001.

Zayed N, Boon N, Bernaerts K, Chatzigiannidou I, Van Holm W, Verspecht T, et al.: Differences in chlorhexidine mouthrinses formulations influence the quantitative and qualitative changes in in-vitro oral biofilms. *Journal of Periodontal Research* 57(1):52-62, 2022.

ABSTRACT (IN KOREAN)

나노불화은이 코팅된 교정용 탄성체의 바이오필름 형성 및 탈회 억제 효과

<지도교수 김백일>

연세대학교 대학원 응용생명과학과

최 준 혁

교정치료 중 브라켓 주변은 바이오필름의 침착이 쉽고, 제거가 어려워서 치아우식증이 호발하는 위험 부위이다. 따라서 본 연구에서는 해당 부위의 바이오필름 침착과 백색 병소의 예방을 위해 나노불화은이 서방형으로 용출되는 교정용 탄성체(Nano silver fluoride sustained-release orthodontic elastomerics; NSF-RE)를 개발하고, 화학적 및 물리적 특성을 확인하였다.

또한 항바이오필름 및 탈회 억제 효과를 평가하여 임상적 활용가능성을 확인하였다.

첫 번째 연구의 목적은 나노불화은을 서방용출하는 최적의 코팅용액 조건을 탐색하고, 코팅용액이 적용된 탄성체의 물리적 특성을 평가하는 것이었다. 두 번째 연구의 목적은 *S. mutans* 에 대한 항균 지속 및 항바이오필름 효과를 평가하는 것이었고, 세 번째 연구의 목적은 다균종 바이오필름에 대한 항바이오필름 및 탈회 억제 효과를 평가하는 것이었다.

첫 번째 연구에서 에틸셀룰로오스와 폴리에틸렌글리콜을 각각 다른 조성으로 혼합한 4 가지 조합의 용액에 딥 코팅 방법으로 교정용 탄성체를 코팅하였다. 제작된 탄성체에 대해 은 나노입자(AgNPs)와 불소의 용출량 및 용출 기간을 평가하였다. 또한 항균 코팅이 탄성체의 인장력에 미치는 영향을 평가하였다. 코팅용액에 에틸셀룰로오스가 포함된 경우, 탄성체 표면으로부터 AgNPs 와 불소 모두 7 일 동안 지속적으로 용출되었다. 누적 용출량 평가 결과, 에틸셀룰로오스와 폴리에틸렌글리콜이 2:1 의 비율로 구성된 코팅용액을 적용한 탄성체(NSF-EP2)는 다른 조성의 코팅용액이 적용된 탄성체에 비해 유의하게 많은 은 나노입자와 불소 누적 용출량을 보였다($P < 0.01$). 한편 코팅 유무 및 코팅용액의 종류에 따른 탄성체 간의 인장력은 통계적으로 유의한 차이를 보이지 않았다.

두 번째 연구에서는 *S. mutans* 에 대한 코팅 탄성체의 항균 지속 및 바이오필름 형성 억제 효과를 평가하였다. 항균 지속 효과는 *S. mutans* 를 도말한 고체 배지 표면에 탄성체를 올려놓고 24 시간 배양한 후, *S. mutans* 가 도말된 새로운 고체 배지로 탄성체를 옮겼다. 동일한 과정일 7 일 동안 반복하고, 7 일 후 배지 표면에 형성된 inhibition zone 을 mm 단위로 측정하였다. 바이오필름 형성 억제 효과는 시편 표면에서 64 시간 성숙된 *S. mutans* 바이오필름에 대해 colony forming units (CFUs)를 확인하였고, confocal laser scanning microscope (CLSM)을 이용하여 바이오필름의 두께와 live/dead cell ratio 를 평가하였다. 그 결과, NSF-EP2 는 가장 큰 inhibition zone 을 보였으며, NSF 및 NSF-E 에 비해 각각 2.64 배, 1.31 배 유의하게 컸다(각각, $P < 0.001$, $P < 0.001$). 바이오필름 평가에서도 NSF-EP2 의 CFUs 는 control 에 비해 57% 유의하게 낮았다($P < 0.001$). CLSM 결과, NSF-EP2 는 control 에 비해 바이오필름의 두께는 83%, live/dead cell ratio 는 96% 유의하게 감소하였다($P < 0.001$). NSF-EP2 의 항바이오필름 효과는 다른 군에 비해 가장 높았다.

세 번째 연구에서는 다균종 dental 바이오필름 모델인 dental microcosm biofilm model 을 이용하여 NSF-RE 의 항바이오필름 및 탈회 억제 효과를 평가하였다. 우치 시편 표면에 바이오필름을 형성시키고, 1 일 간격으로 총 7 일 동안 QLF 를 이용한 바이오필름의 성숙도(Red/Green ratio; R/G ratio)를

평가하였다. 바이오필름 형성 7일 후 CFUs를 이용하여 cell viability를, CLSM을 이용하여 바이오필름의 두께와 live/dead cell ratio를 평가하였다. 바이오필름 형성 3일, 7일차에 NGS를 이용한 미생물 조성의 변화를 평가하였다. 탈회 억제 효과는 7일 동안 성숙된 바이오필름 하방의 법랑질에 QLF를 적용하여 mineral loss (ΔF, ΔF_{max})를 평가하였다. 탄성체로부터 용출되는 유효물질의 작용 거리는 시편에 부착된 탄성체로부터의 거리에 따른 법랑질의 ΔΔF로 평가하였다. 평가 결과, 에틸셀룰로오스와 폴리에틸렌글리콜이 2:1로 구성된 코팅용액을 적용한 탄성체(NSF-EP)의 R/G ratio는 control에 비해 3일차부터 유의하게 낮은 값을 보였다(P = 0.013). Cell viability 평가 결과, CFUs는 control에 비해 total bacteria에서 9.4%, aciduric bacteria에서 13.0% 유의하게 감소하였다(각각, P = 0.001, P = 0.03). CLSM 평가 결과, 바이오필름의 두께는 36.1% 유의하게 낮았으나(P = 0.036) live/dead cell ratio는 유의한 차이를 보이지 않았다. 바이오필름 성숙 3일, 7일 차에 치아우식과 관련 있는 것으로 알려진 5종의 박테리아(*S. mutans*, *L. fermentum*, *V. dispar*, *V. atypica*, *V. parvula*)에 대한 상대풍부도의 총합은 NSF-EP에서 가장 낮았다. NSF-EP의 ΔF와 ΔF_{max}는 control과 비교하여 각각 34.8%, 38.7% 유의하게 높았다(각각, P < 0.001, P = 0.001). 시편 내 탄성체로부터 거리에 따른 ΔΔF는 유의한 차이를 보이지

않았다. AgNPs 와 불소의 누적용출이 가장 많았던 NSF-EP 는 모든 평가항목에서 가장 항바이오필름 및 탈회 억제 효과를 보였다.

결론적으로, 본 연구는 나노불화은으로 코팅된 새로운 교정용 탄성체가 AgNPs 및 불소를 7 일 동안 지속적으로 용출함으로써 다균종 바이오필름 형성 및 백색 병소 예방에 유의미한 효과를 제공할 수 있음을 확인하였다.

핵심되는 말: 나노불화은, 약물 전달 시스템, 항우식, 교정용 탄성체